IEEE Access
Multidisciplinary | Rapid Review | Open Access Journal

Received 3 December 2024, accepted 19 December 2024, date of publication 26 December 2024, date of current version 7 January 2025.

Digital Object Identifier 10.1109/ACCESS.2024.3523401

RESEARCH ARTICLE

Augmenting Energy Sustainability of Static Nodes Using Hybrid KGNN-AHP Driven Approach for IoT-Based Heterogeneous WSN

R. BLESSINA PREETHI AND M. SARANYA NAIR
Vellore Institute of Technology, Chennai 600127, India
Corresponding author: M. Saranya Nair (saranyanair.m@vit.ac.in)

ABSTRACT As the nodes used in Internet of Things (IoT)- based wireless sensor network (WSN) are constrained by the limited source of energy, contemporary applications incorporate the heterogeneous energy model WSN. Although the node energies are heterogeneous in application, further study is required to improve the potential of heterogeneous WSN and not much is explored on Graph Neural Network (GNN) clustering and Routing methods, which impels this study on novel optimal clustering of nodes with efficient cluster head selection and routing for heterogeneous WSN. In the proposed work, a novel clustering model with K-nearest neighbour (KNN) and GNN clustering, followed by the Analytic Hierarchical Process (AHP) weight-based cluster head (CH) selection method to find the optimal and eligible CH with classified fitness functions. The chosen parameters for the fitness functions are the base station to node distance, lifetime of the nodes in the network, average number of neighbouring nodes in the cluster, peak power transmission by the node in the network, and the average lifetime of nodes in the cluster. Additionally, the proposed algorithm ensures the eligibility of the optimal relay nodes using the GNNSage based routing and steady-state of data transmission from source nodes to the base station. As the model is designed for static nodes deployment for monitoring environmental changes in realtime application. The simulation results exhibit the enhancement of network lifetime and data transmission by following the proposed algorithm for static network.

INDEX TERMS Analytic hierarchical process, graph neural network, GraphSAGE, heterogeneous WSN, Internet of Things.

I. INTRODUCTION

Technological development in exploring a region of interest (RoI) and gathering information to predict the future is increasing day by day. The necessity of gathering information is partially met by the contemporary Internet of Things (IoT). IoT is extremely cooperative and interconnected with multifarious bodies such as Wireless Devices, Humans, Animals, and other living or non-living things, but the IoT does not adopt an explicit communication paradigm, hence wireless communication technologies play a significant part in the roll-out of IoT [1]. Wireless communication technology is efficiently employed by wireless sensor networks (WSN) to reinforce the IoT-based real-time applications in the fields of Industry, Smart Agriculture, the Health sector, Environmental Monitoring, Military, and Surveillance. The WSN is the mainstay of IoT in the perception layer of communication systems for gathering environmental information from sensory nodes and forwarding the data through various modes to the IoT network [2].

As the usage of WSN has increased in various applications, such as weather, underwater, industrial, space monitoring, and health monitoring, the energy consumed by these devices is increasing daily. IoT-based WSNs are embraced with multitudinous sensor nodes constrained by batteries and power sources [3]. The tiny batteries of sensor nodes exhaust within a short span of time owing to processing and communication, and the battery of the sensor nodes is

The associate editor coordinating the review of this manuscript and approving it for publication was Adamu Murtala Zungeru.

non-renewable or irreplaceable when the nodes are deployed in hazardous and non-human allowable areas. Hence energy efficiency and lifetime enhancement of the network are substantial goals in designing a productive network. The enhancement of energy efficiency in sensor nodes is a crucial aspect in the augmentation of the network lifetime. The algorithms proposed for an optimal method of delivering packets, efficient routing, security, and coverage of the network alleviate the finite battery of sensor nodes and expire the network early. Therefore, the energy-efficient algorithms in the field of IoT-based WSN is in demand to extend the network lifetime [4].

Various researches have been conducted to address the problem of extensive energy consumption and effective utilization of battery resources of sensor nodes in IoT-based WSNs. The major fields of research in energy magnifications are data reduction, radio optimization, efficient routing, duty cycle schemes, and battery replenishment. In the data reduction method, the algorithms are used to control the redundant data transmission and qualify the data aggregation and data compression to reduce the energy consumption of the network for the recurrent transmission of redundant data [5]. The Radio Optimization method proposes the transmission power control, cooperative communication, and directional antennas which reduce the energy utilized by the devices for communication. Another process of an energy optimization in the network is efficient routing by multipath routing schemes, sink mobility, relay node deployment, and clustering. The duty cycling method is used on the nodes to be in an active and sleep state for reducing the power consumption during idle listening. However, the tiny smart sensors are embedded in the nodes of monitoring as a result, the size of the node decreases then the battery power utilized will also be decreased. This seems to be a good solution for energy consumption in WSN but the nodes squander their energies for the processing, transmission, and reception of data. Hence, the insubstantial sources used for battery replenishment in a node and the authors surveyed the natural and artificial energy harvesting methods [6], [7]. Energy is harvested from solar power, thermal variation, mechanical vibrations, wind swirls, water drifts, and radiofrequency/electromagnetic fields, and those energies are stored in rechargeable batteries, and super-capacitors or utilized promptly [8]. The constrained battery problem can be solved by the energy harvesting technology but the components embedded in the node for harvesting also make the device design complex and expensive. Variegated techniques have been proposed to decline the depletion of energy in sensor nodes, which encompass power-efficient routing protocols, sleep and wake-up duty cycles, data reduction techniques, radio optimization techniques, and wireless power and information transmission technologies despite the efficient clustering in hierarchical networks being more effective than other methods [9]. The Hierarchical network follows the layering model in which the sensor nodes are grouped into a cluster and among them, one is selected as the cluster head or relay node to forward the data to the sink by finding the next node with higher energy. Clustering is the most energy-efficient technique followed by densely deployed networks [10]. Every cluster has a single cluster head (CH) or dual cluster head used to aggregate the sensed and forwarded data from the member nodes in the cluster. The CH has a higher responsibility than the member nodes, it has to gather the data from the member nodes, eliminate the redundant data, and forward it to the base station (BS)/sink node. This transmission can be done directly from CH to BS or through multi-hop from one CH to another CH until the data reaches the Base Station. Clustering is appreciated because of the high reduction in energy consumption according to the maximum power transmission theory. Clustering of the nodes is performed by either the temporal or spatial correlation of homogeneous nodes but this is not feasible for the network deployed with heterogeneous wireless sensors.

The optimum clustering model and energy-efficient cluster head selection in homogeneous WSN is handled by formulating a novel weighted method using bio inspired algorithms. The weight-based fitness function is used by the protocol to segregate the nodes according to their eligibility value to become a cluster head or a member node in a cluster. A mathematical model for formulating the fitness function and random weighted average is defined and stated for an energy efficient and secured network [11].

Existing algorithms are unable to handle the node heterogeneity characteristics that directly affect network lifetime. Hence the significant characteristics of the heterogeneous nodes are given priority while assigning weights to the analytical hierarchical process. Obtain a cost-effective and optimized solution to determine which prioritized attribute contributes more to the enhancement of node life and network lifetime.

The motivation for this research is driven by the critical need to enhance the energy efficiency of wireless sensor networks (WSNs), given their limited operational lifespans and data transmission capabilities due to energy constraints. As WSN applications evolve, the shift from homogeneous to heterogeneous energy models presents new challenges and opportunities. The heterogeneous energy models enable better adaptation to nodes with varying energy capacities,which requires further exploration to optimize the networks for practical use. Moreover, the Graph Neural Network (GNN) clustering and routing methods offer promising benefits for WSN management, their application within this domain is still relatively evolving. This research aims to bridge these gaps by investigating how GNN-based clustering and routing can be effectively integrated with heterogeneous energy models, thus advancing both the adaptability and efficiency of WSNs in real-world scenarios.

The proposed model integrates Graph Neural Networks (GNNs) for clustering, weight-based cluster head selection, and Graph Sage algorithm for routing in IoT-based

TABLE 1. Table of acronym.

Acronym	Definition
AD	Advance Nodes
AHP	Analytical Hierarchical Process
AND	All Node Dead
ARE	Average Residual Energy
BS	Base Station
CH	Cluster Head
DEEC	Distributed Energy Efficient clustering
DWEHC	Distributed weight-based energy-efficient hierarchical clustering protocol
EEHCT	Energy-Efficient Hybrid Clustering Technique
FND	First Node Dead
FSMO	Fuzzy Spider Monkey Optimization
GLDs	gain and loss
GNN	Graph Neural Network
HEED	Hybrid Energy Efficient Distributed Clustering
HLEACH	Heterogeneous LEACH
HMM	Hidden Markov Model
IoT	Internet of Things
KNN	K-nearest neighbour
LAN	Land area network
LEACH	Low-energy adaptive clustering hierarchy
LEACH-T	Threshold-based LEACH
MOBGWO	multi-criterion binary grey wolf optimizer
MPTCP	Multipath TCP
NN	Node Network
NOR	Normal Nodes
O-LEACH	Orphan-LEACH
SA-LSA	Simulated Annealing with Lightning Search Algorithm
SEP	Stable Election Protocol
TB-LEACH	Time-based Cluster-Head Selection Algorithm for LEACH
TFNs	Triangular Fuzzy Numbers
TOPSIS	Technique for Order Preference by Similarity to Ideal Solution
TSA-DCSO	Turtle Search Algorithm-Desert Cat Swarm Optimization
VH-LEACH	Vice Cluster Head -LEACH
V-LEACH	Vice-LEACH
WSN	Wireless Sensor Network

TABLE 2. Table of symbols.

Symbol	Definition
E_{elec}	Energy consumption per bit by electronic circuits
(x, y)	Location dimension of nodes
E_{amp}	energy used to amplify the sensed data
ε_{mp}	multi-path model
E_{ad}	Energy consumed to aggregate the sensed data
$E_{TX}(l, d)$	consumption of energy for transmitting a bit
$E_{RX}(l, d)$	consumption of energy for receiving a bit
l	Size of packet
d_o	Distance threshold
C_M	Total number of member nodes in the cluster
$E_{CH-TX}(l, d)$	consumption of energy in CH for transmitting a bit
$E_{CH-RX}(l, d)$	consumption of energy in CH for receiving a bit
k_{opt}	Optimal number of clusters
N	Number of nodes in the network
A	Nodes deployed area in square meters
μ	fraction of advanced nodes
E_{T-NOR}	Total Energy of Normal nodes in network
E_{T-AD}	Total Energy of Advanced nodes in network
E_0	Initial Energy of Node
$\mathbb{V}$	Vertice
$\mathbb{E}$	Edge
$\mathbb{G}$	Graph
$\mathbb{F}$	Features of nodes
ω	Weights
m_v	Member nodes of node v
$c(u, v)$	Cluster comprices node v and its neighbour u
h_n^l	Hidden state of a node in layer l
σ	activation function
b	bias
(S_c)	silhouette score
L_c	Loss function
D_{N-BS}	Distance from node to BS
CH_l	Lifetime of a CH
N_N	Average intra-cluster distance
f_v	Fitness Value
r	Relay node
R	Set of Relay nodes

heterogeneous WSN. Initially, the network nodes are organized into clusters using GNNs, leveraging their ability to capture complex relational structures within the network. GNNs facilitate the clustering process by considering the connectivity patterns and interactions among nodes,thereby enabling the identification of cohesive groups based on their topological characteristics. Following clustering, a weight-based approach is employed to select cluster heads, where nodes with higher centrality or importance within each cluster are prioritized for the role of cluster head using an Analytical Hierarchical Process (AHP). This selection mechanism ensures efficient coordination and management of intra-cluster communications, enhancing network performance and resource utilization. Subsequently, routing decisions are made using the Graph Sage algorithm, which leverages node embeddings and graph convolutions to learn the representations of the network topology. By incorporating contextual information and neighbourhood relationships,the Graph Sage enables intelligent routing decisions that optimize communication paths while considering factors such as distance, link quality, and energy efficiency. Overall, the proposed model offers a comprehensive approach to WSN management by combining GNN-based clustering, weight-based cluster head selection, and Graph Sage routing to achieve enhanced network efficiency, scalability, and resilience in dynamic and heterogeneous environments.

This paper is organized with an Introduction to WSN and a brief note on the heterogeneous WSN clustering method used in this process, followed by a literature review related to the work briefed in Section II. Section III briefs the system model with assumptions and Section IV explains the proposed work from initialization to data transmission and the algorithm. Section V discusses the simulation results and Section VI to conclude the paper.

II. RELATED WORK

This section discusses the work performed in relation to the proposed model. Initially, heterogeneity is termed the network deployed with nodes that vary in computational processing, link level heterogeneity, or energy heterogeneity. In computation heterogeneity, the node must be instructed to process multiple tasks at a time by using the central processing unit and the graphical user interface or the nodes may vary in memory, which means computing the node with multiple sources create network heterogeneity in computation [12], [13]. Link heterogeneity varies according to the communication channel or medium used in the network of sensor nodes for communication. As there are two models of communication, a land area network (LAN),

and a wide area network (WAN), used by the nodes to communicate with each other either by a combination of wired and wireless high bandwidth channels for the longer distances the network is known under the link heterogeneous network [14]. The energy heterogeneity in a network is that the nodes deployed in the ROI have different nth levels of initial energy [15]. In the early stages of development, the WSN was totally concerned with the homogeneous sensor nodes deployed network that diverges as centralized, decentralized, and ad hoc, so the protocols were designed on this concern but the Heterogeneous LEACH (HLEACH) protocol brought the clustering hierarchy and the random selection of CH in the Heterogeneous network [16]. Though the LEACH is an efficient protocol, it elects the cluster head randomly and considers the nodes to be homogeneous in initial energy. Even in the B-Leach protocol the nodes are homogeneous in energy and the CH selection is uniform in all rounds which makes a high overhead [17]. The I- Leach is the modified protocol of LEACH to overcome its limitation by electing the CH based on its residual energy and location [18]. Furthermore, Leach-based protocols such as V-LEACH, VH-LEACH, LEACH-T, and TB-LEACH have proven their energy efficiency network but these are all simulated on the homogeneous network [19], [20], [21], [22]. Though the HEED [23] protocol has better efficiency than the LEACH, the HEED is also designed for a homogeneous network.

A Stable Election Protocol (SEP) is proposed for the energy two-level heterogeneous WSN and it is termed the nodes as advanced nodes, and normal nodes. The advanced nodes are deployed in m fraction of normal nodes and they have α times higher energy than normal nodes [24].

The improved version of the H-Heed protocol increased the level of energy heterogeneity and proved that the level of energy heterogeneity increases the network lifetime. These protocols do not consider the diverse parameters of the CH during the election process [25]. They contemplate that the energy of all the nodes is equal at the end and beginning of a new round, hence the prospect of sensor nodes becoming CH is equal to all. This is taken into deliberation for forming the Distributed Energy Efficient clustering (DEEC) protocol [26]. The DEEC protocol formulates a novel probability for the heterogeneous nodes to become the CH and the study shows that the probability of becoming a CH is high for the advanced nodes when compared with normal nodes and this is the major flick to extending the network lifetime. As the probability of selection is a unique concept but the nodes are eligible to become the CH, it is rejected if it's already selected as CH. Therefore, this is solved by the weight-based cluster head selection method in which multiple parameters are used to rank the node that has the least rank will be selected as CH [27] Sandip et al. have proposed an Energy-Efficient Hybrid Clustering Technique (EEHCT) to cluster the nodes. The cluster is designed in two different modes such as dynamic clustering and static clustering. The balanced cluster energy is evaluated and according to the energy level of the cluster, the BS decides whether to declare the cluster to be static for the rest of the rounds or dynamic [28].

L Sahoo et al. have proposed two decision-making methods in which the entropy-weighted technique and the Technique for Order Preference by Similarity to Ideal Solution (TOPSIS) method based on Triangular Fuzzy Numbers (TFNs) are used. In the entropy-weighted technique, criteria weights are determined based on the information-carrying capacity of each criterion and assessed using entropy values. These weights are calculated through a four-step procedure involving the examination of a decision matrix and the normalization of values. However, it may be computationally intensive and sensitive to variations in data. On the other hand, the TOPSIS method under uncertainty incorporates uncertainty using TFNs. This involves defining criteria and alternatives, normalizing TFNs, weighting criteria, creating a normalized decision matrix, determining ideal and non-ideal solutions, calculating similarity to ideal and non-ideal solutions, computing relative closeness, and ranking alternatives based on their relative closeness. Both methods provide systematic approaches for multi-criteria decision-making, offering insights into the relative importance of criteria and facilitating the selection of preferred CH and density-based clustering model [29].

Most of the protocols follow the procedure of CH selection, declaration of CH and formation of cluster, and routing. Hongzhang Han et al. have designed a routing protocol based on ant colony optimization model in WSN [30]. As the data transmission is directly proportional to energy consumption, the selection of node in the routing is highly dependent on energy and link quality. Here the link quality is estimated by the traffic of nodes for transmitting data from the source node to the target node. The authors stated that nodes located near each other have a very low probability of packet loss, which also increases the energy of the node. Mishra SD et. al have introduced a method called reliable clustering with optimized scheduling and routing for wireless sensor network, which employs GridCosins chain clustering to form distance tree topology-based chaining of sensor nodes. Additionally, it introduces a Turtle Search Algorithm-Desert Cat Swarm Optimization (TSA-DCSO) for CH selection. However, it acknowledges the limitations of current methodologies, such as unexpected sensor node failure due to channel congestion and mutual interference during data transmission. To address this, it proposes a Decisive Scheduling Optimized communication cost routing that considers energy levels and round-trip delay time for decision-making.A potential limitation of the approach is the increased computational overhead due to the integration of multiple optimization algorithms, which could affect real-time responsiveness in dynamic network environments. [31] In a large network, the low energy adaptive clustering hierarchy that enables direct transfer from CHs to the base station is impractical. To address this, Senthil et al. have proposed an optimized Orphan-LEACH (O-LEACH)

protocol, and simulated annealing with Lightning Search Algorithm (SA-LSA) to efficiently utilizing orphan nodes to cover the network [32]. The O-LEACH proposes two solutions: firstly, a cluster member can act as a gateway, creating a floating node within the cluster. This gateway node, which serves as the CH, can handle multiple orphan nodes' communications, aggregating data and forwarding it to the BS. Secondly, in cases where there is a non-secure area with essential stranded nodes outnumbering node losses in the cluster, a new CH is created. This new CH, designated as CH, takes on the role similar to that of the original CH. However, a limitation of this approach may arise from the complexity of managing orphan nodes and optimizing the network coverage. Even the paper [33] considered the residual energy of the nodes and the distance between the nodes. The authors have considered the nodes as quasi-stationary and location-aware nodes with the embedded GPS or by the reception of signal strength or by the direction of location in the form of x,y concerning the base station or the neighbouring nodes. The authors have introduced the DWEHC protocol. In the initialization stage, all sensor nodes forward their location in terms of (x,y) to all nodes under their signal strength. Every node receives a set of neighbouring nodes' locations and it has to calculate the distance between itself and the neighbouring nodes using a mathematical formula and tag itself as `my_level = -1`. This -1 is the indication that the node has not yet joined any cluster. After finding the distance, the nodes need to forward their estimated value of distance which is considered as one of the weighing factors as `my_weight` to the base station. Then `my_weight` is evaluated in the base station and the largest neighbour node with the highest energy will be elected as a temporary parent node and the other nodes are termed as child nodes for gathering the information and forwarding it to the recently elected parent node. Subsequently, the temporary parent node must be acknowledged by its child node to become a permanent parent node to form the cluster. Huangshui Hu et al. introduced a clustering routing protocol named PFCRE which leverags fuzzy logic and particle swarm optimization techniques to enhance energy efficiency, mitigate energy holes, and extend the network lifespan. PFCRE prioritizes energy minimization and balance in cluster formation through an enhanced particle swarm optimization algorithm. Additionally, it incorporates a fuzzy inference system to determine the optimal routes for the CH, considering factors such as residual energy, distance to the base station, and relay selection frequency. The PFCRE adopts an adaptive maintenance mechanism to manage clusters dynamically, eliminating the need for periodic clustering and reducing computation and message overheads. While PFCRE shows promising results in improving energy efficiency and extending network lifespan, its effectiveness may be limited in highly dynamic network environments where node mobility or varying traffic patterns could challenge the stability of the clustering structure [34]. Yuebo L et al. have proposed a fuzzy clustering model to select the CH with three parameters namely residual energy, node degree deviation, and distance to centrality, which are regarded as fuzzy inputs. After selection of the CH, a cluster is formed based on the signal strength and fuzzy based routing is generated. The routing of the data is chosen by the eligible nodes residual energy, node degree to the mean number of neighbours of all the node, and the distance of the node to the centrality of its neighbours. This fuzzification involves approximately 75 combinations of IF-THEN rules to optimize routing decisions. While the fuzzy clustering model presents a comprehensive approach to CH selection and data routing, its performance may be affected by the complexity and computational overhead associated with managing a large number of IF-THEN rules. Additionally, the effectiveness of the model can be influenced by the accuracy and reliability of the input parameters, particularly in dynamic network environments where conditions may change rapidly [35]. Pal R et al. have proposed a multi-criterion binary grey wolf optimizer (MOBGWO) based clustering method for heterogeneous wireless sensor networks [36]. There are five objectives namely, maximizing overall cluster head energy, minimizing cluster compactness, minimizing the number of cluster heads, minimizing energy consumption from non-cluster head to cluster head transmission, and maximizing cluster separation. An equal weight distribution leads to a linear combination that transverses multiple objectives into a single objective. To overcome this problem in weight assignment the authors have infused the Pareto optimal formulation solution which retains the diversity of the objectives and the authors also discussed the MOBGWO method which converts the multiple objective functions into single objective function.

Mingwei Lin et al. [37] have proposed a new method for assigning weights to the functions. They set the ordered weighted averaging (OWA) of the input values with the aid of the probability density function (PDOWA). The probability density function, the inputs to be taken for consideration, are arranged in descending order, and kernel density estimation is applied to estimate the probability density function to determine the structure of the cluster to be formed by the input values. The Kernel function has three models such as Gaussian, uniform and Epanechnikov kernel mathematical models, among these the authors have chosen the general classic Gaussian model of the kernel function to estimate the probability density function of the inputs to be assigned with weights, which can also identify the local cluster structure of given input values of the real-time case study.

Liu Z et al. conducted node failure analysis using a weight factor. They have analyzed the Failure Mode and effect analysis (FMEA) which is used in management technology with normal risk priority number (RPN) and has several drawbacks when implementing in an application [38]. Hence to overcome the drawback, they have proposed weight-based probabilistic linguistic preference relations (PLPRs) with the score evaluated by the gain and loss (GLDs). GLD is used

to derive the risk ranking of the failure nodes in the network. They have taken both the individual modes' risk ranks and the group modes' risk ranks to identify the optimum risk value in the network. At last, they evaluated the load haul dumper machine risk with the weight calculated using the analytical hierarchical process (AHP).

AHP is a powerful tool for qualitative and quantitative analysis of the multiple attributes to make appropriate decision on relative weights. The basic ideology of eliciting judgments by decision makers on closely or diversely related attributes is based on weightage [39]. The AHP makes judgments and calculations better by comparing the weights. The theory of AHP is derived from the process of candidate selection for a job by evaluating the skills and other contributions of the employees with a weighted average [40]. Herein, CH selection in a heterogeneous network is also a multi-attributive problem, where the order of priority in attributes and related weight selection is complex. Hence, the problem is addressed in the proposed model by incorporating the initial stage of weight election with AHP and Ranking.

Arif et al. have proposed a framework integrating Fuzzy Spider Monkey Optimization (FSMO) and a Hidden Markov Model (HMM). The protocol rounds consist of setup and steady-state phases. In the setup phase, CH selection is simplified using SMO to construct energy-efficient clusters based on network remaining energy and non-overlapping distance. During the steady-state phase, CHs gather data from cluster members and transmit it to the base station (BS). However, a drawback of this model is the complexity introduced by integrating FSMO and HMM, which potentially increases the computational overhead. Additionally, relying solely on SMO for CH selection during setup may not always result in optimal cluster configurations, leading to suboptimal energy efficiency in certain scenarios [41].

In the described model, cluster head selection follows a hierarchical approach initiated by the base station transmitting a BS_Init_msg to initialize clustering. the top layer nodes receive this message, determine their distance from the base station and participate in cluster head competition. Each top layer node broadcasts a start_msg containing its ID, distance to the base station, remaining energy, and prediction energy, exchanged with neighbouring nodes to facilitate cluster head selection. Nodes evaluate their weighted election for cluster heads based on predefined equations, considering factors such as the energy level, distance to the base station, and prediction energy. Cluster heads are selected based on higher weighted scores, favoring nodes with greater energy reserves, shorter distances to the base station, and high prediction energy. Once selected, the cluster heads update the distance information for each network level and exchange local information with nearby nodes to optimize routing paths. This iterative process continues to facilitate efficient data transmission and network performance [42].

S. He et al., provide a detailed overview of the methods employed for constructing Wireless Communication Graphs (WCG) in various network types, including mesh/ad-hoc networks, cellular networks, and wireless local area networks (WLANs). They elaborate on the methodologies used to establish these communication graphs, shedding light on the intricacies involved. Additionally, the authors introduce classical paradigms of Graph Neural Networks (GNNs) applied within wireless networks, aiming to enhance the comprehension of GNN concepts and structures. Through their review, they offer a comprehensive examination of GNNs utilized in wireless networks, covering diverse areas such as resource allocation and emerging fields. This review contributes to a deeper understanding of the existing directions and potential applications of GNNs in wireless communication systems [43].

Ting Zhu et al. have proposed a model for Multipath TCP (MPTCP) to enhance network utilization in 5G networks. MPTCP extends TCP to enable concurrent packet transfer over multiple paths by utilizing cross-layer optimization techniques such as routing and path management. However, existing multipath routing algorithms face the challenge of subflow asymmetry due to network heterogeneity, which limits comprehensive routing optimization. To address this, the paper [44] introduces a novel Graph Neural Network (GNN)-based multipath routing model to explore the link, path, subflow, and MPTCP connection complexities. Leveraging the GNN model, expected throughput can be predicted,thereby guiding multipath routing optimization. Despite its advancements, a potential drawback of the model is the increased computational complexity associated with GNN-based routing optimization, potentially impacting real-time performance in large-scale networks [44].

However, the existing algorithms such as HLEACH, B-LEACH, SEP, DEEC, and HEED have made significant advancements in energy efficiency and clustering for WSNs, which are regularly suitable primarily for homogeneous networks or apply simplistic clustering techniques that may not fully exploit the heterogeneity within WSNs. Multi-criteria decision-making techniques used in algorithms of EEHCT and optimization-based approaches such as TSA-DCSO, SA-LSA, and GNN-based models have introduced more sophisticated methods for cluster head selection and energy balancing. However, the TSA-DCSO and MOBGWO are the metaheuristic search algorithms used in fitness functions based optimal CH selection without explicit prioritization of criteria by treating all parameters as equally or randomly significant. Though this models simplify the optimization process, it may not give the best CH selection when certain criteria are precedence over others. In the Proposed model, AHP specifically addresses this limitation by structuring the CH selection process around prioritized weights. AHP ensures that the critical factors have a greater influence on CH selection, leading to more optimal and contextually relevant results by explicitly ranking criteria according to the priority. Moreover, the weight based and optimization algorithms are designed for high-performance optimization

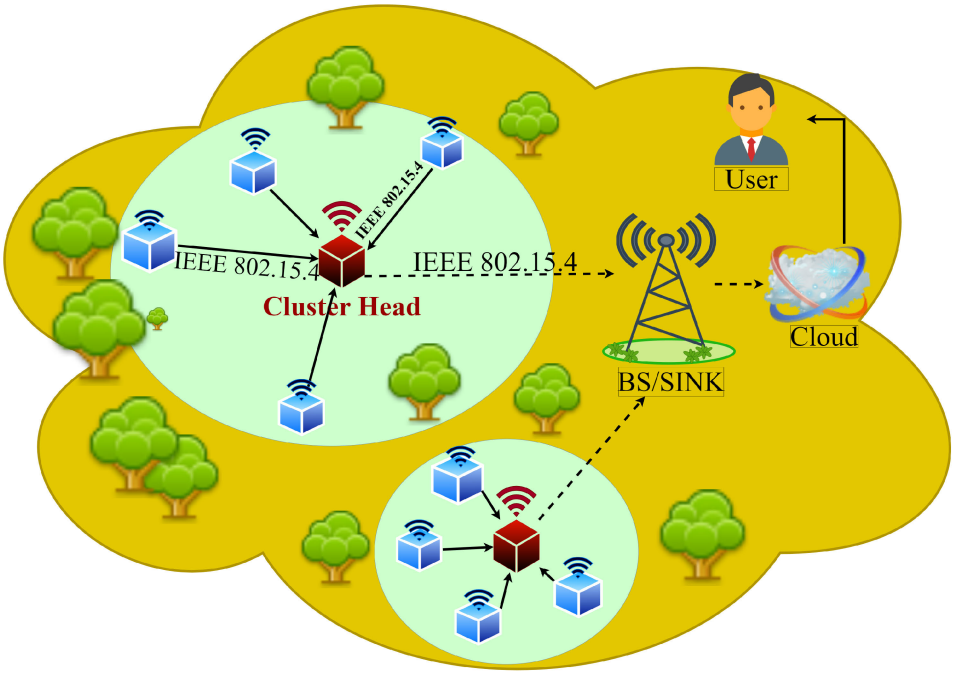

FIGURE 1. IoT based WSN Architecture.

which involves significant computational complexity in large networks with complex fitness functions. Therefore, AHP incorporates explicit calculations and comparisons, which are computationally less intensive than evolutionary algorithms, hence AHP based CH selection is highly recommended for real-time applications where rapid CH selection is needed. Furthermore, many of these models lack an integration of advanced clustering and routing techniques tailored to heterogeneous WSNs, which limiting the adaptability to real-world applications.

III. SYSTEM MODEL

A. MODEL ARCHITECTURE

Figure 1 illustrates an IoT-based Wireless Sensor Network architecture which consists of multiple sensor nodes, each equipped with IEEE 802.15.4 wireless communication modules. The IEEE 802.15.4 protocol is specifically designed for low-power, low-data-rate applications, making it ideal for WSNs where energy conservation is crucial. The IEEE 802.15.4 standard supports a simple and robust communication framework, enabling reliable data transmission between the sensor nodes and the Cluster Head within the limited range and power constraints of typical WSN deployments. These nodes are organized into clusters, with a designated cluster head responsible for coordinating communication and data aggregation within the cluster. The cluster heads then relay the aggregated data to a Base Station (BS) or Sink, which acts as a gateway to connect the WSN to the cloud [45].

The IoT standards, IEEE 802.15.4 is employed as a key protocol for communication within the WSN. This standard is widely recognized in IoT deployments for enabling low-power, low-data-rate communication among devices, which is essential for battery-operated sensor nodes. For internet connectivity, the architecture utilizes a variety of IoT-related standards depending on the specific deployment. For instance, connectivity to the cloud from the BS can be achieved via Wi-Fi (IEEE 802.11), cellular networks (4G/5G), or Ethernet. The cloud connection facilitates data analysis and decision-making processes.

This hierarchical architecture enables users to monitor the network remotely and access real-time data through cloud services. In this architecture, the IoT and WSN are closely integrated, as the sensor nodes gather environmental data and transmit it through a Cluster Head (CH) to a BS, which then sends it to the cloud. The architecture leverages IoT principles, enabling remote monitoring, data accessibility, and real-time analysis through cloud connectivity. The IoT framework here ensures that data collected from physical sensors can be processed and accessed over the internet, bridging the physical network (WSN) with digital services (IoT). This integration aligns with IoT goals, providing a seamless pathway for data to travel from sensor nodes to end-users. The cloud connection facilitates data analysis and decision-making processes, supporting various IoT applications such as precision agriculture, environmental monitoring, and smart cities and healthcare.

The proposed method for energy-efficient clustering and cluster head selections is implemented in a network area where the sensor nodes are heterogeneous in nature. Heterogeneous sensor nodes are classified into two categories as Normal Nodes (*NOR*) and Advanced Nodes (*AD*). The deployment of normal nodes are in random order to cover

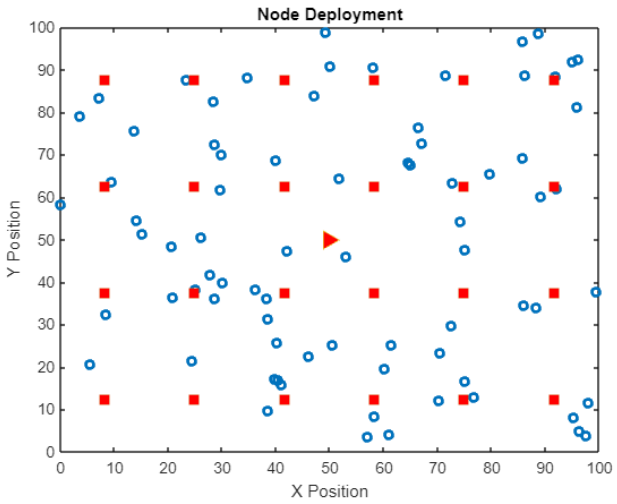

FIGURE 2. Deployment of Heterogeneous Nodes.

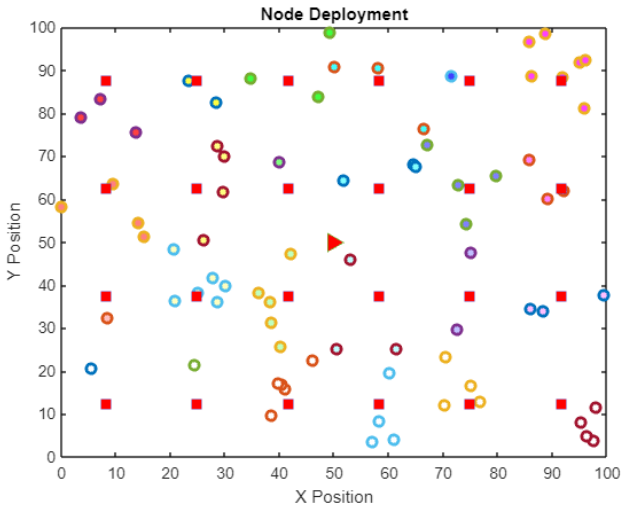

FIGURE 3. Clusters of heterogeneous nodes.

the entire region of deployment (RoD) and Advanced nodes disseminated uniformly inside the equivalent geological area of the normal nodes as shown in Figure 2. The nodes are formed into an optimal number of clusters using KGNN, a weight-based cluster head selection method is used to select the appropriate cluster heads in the network, and the other nodes are treated as member nodes. The scenario of the proposed model is shown in Figure 3. The nodes are allowed to transmit sensed packets after the declaration of the cluster head in a cluster. The cluster heads receive packets from the member nodes and forward the packets to the BS/sink node.

B. BASIC ASSUMPTIONS IN PROCESSING NETWORK DESIGN

- Iot based WSN nodes are heterogeneous in energy and the network has two-level energy heterogeneous nodes.
- The fraction of normal nodes is higher than the advanced Nodes
- The nodes that have an initial energy equal to Eo are considered normal nodes and those with energy $>$ Eo are considered advanced nodes.
- All the deployed nodes are static in nature, hence the nodes are known for their location in dimensional (x, y).
- Every node is allotted a unique ID, and that is maintained for the entire process of assessment.
- Every member node is capable of sensing the environment and forwarding data to the CH and the CH forwards the data to the BS.
- Links are symmetric that is the transmission power between two nodes is equal.
- The time synchronization of the nodes are ideal.
- Consideration of a node dead state is only when the total energy of the node is depleted $(E = 0)$.
- The nodes are under the direct control of a static BS which acts as gateway and connected to cloud.
- The BS has uninterruptible energy.

C. SYSTEM MODEL TIMING

The process of execution starts from initialization and ends once all the nodes are dead or reach maximum rounds. Herein, the system timing is defined in several rounds. A round is the duration of the sensed packets traveling from node to the cluster head and from CH to BS. The packets are forwarded by the principle of non-persistent Carrier Sense Multiple Access (CSMA). The data transmitted by the nodes does not interfere with the data of other nodes.

D. ENERGY MODEL OF NODES FOR COMMUNICATION

The Energy of the sensor nodes is spent on basic three processes: (i) data transmission (ii) data reception and (iii) data aggregation. The energy consumption of a node is estimated by the total energy used for transmitting a bit, aggregating data received, and receiving a bit. The total energy consumed by a node is given as the sum of the energy consumption of the radio-electronic sensory circuit for sensing (E_{elec}), energy used to amplify the sensed data for transmission (E_{amp}) for free space model (ε_{fs}) and multipath model (ε_{mp}), energy consumed to aggregate the sensed data (E_{ad}), consumption of energy for transmitting $(E_{TX}(l, d))$ and receiving $(E_{RX}(l, d))$ a data l bit over the distance d [46]. If the d is less than or equal to the threshold (d_o), the d is squared, else the d is taken as d^4.

$$E_{TX}(l, d) = \begin{cases} (E_{elec} \times l) + (l \times \varepsilon_{fs} \times d^2) & ford \leq d_o \\ (E_{elec} \times l) + (l \times \varepsilon_{mp} \times d^4) & ford > d_o \end{cases} \tag{1}$$

$$E_{RX}(l, d) = (E_{elec} \times l) \tag{2}$$

The threshold distance is calculated using the following equation(3)

$$d_o = \sqrt{\frac{\varepsilon_{fs}}{\varepsilon_{mp}}} \tag{3}$$

In the CHs, an amount of energy is consumed for the received data aggregation (E_{ad}), and the energy is also summed with

the total energy consumption of the CHs. The energy spent by the CH is given in Equations (4) and (5), where the C_M is the total number of member nodes in the cluster.

$$E_{CH-TX}(l,d) = C_M \times E_{TX}(l,d) \tag{4}$$
$$E_{CH-RX}(l,d) = C_M \times E_{RX}(l,d) \tag{5}$$
$$E_{CH-TOT}(l,d) = E_{CH-TX} + E_{CH-RX} \tag{6}$$

E. OPTIMAL NUMBER OF CLUSTERS

In the initial setup state, the sensor nodes are grouped into clusters according to the distance between the nodes. The Optimal number of clusters must be chosen in the setup state which avoids the problem of improper clusters, heavy load to CHs, and early dying of CH due to more neighbouring nodes. Thus, determining the optimal number of clusters plays a vital role in energy optimization techniques. It is essential to find the optimal number of clusters that is efficient in minimizing the utilization of average energy and duly distributed total energy consumption among all the nodes in the cluster. Optimal clustering depends on the energy model of the transmitter and receiver distance, number of nodes, and area of deployment. Hence we used the basic radio energy dissipation model to determine the optimal cluster.

$$k_{opt} = \sqrt{\frac{N}{2\pi}} \sqrt{\frac{\varepsilon_{fs}}{\varepsilon_{mp}}} \frac{M}{d_{BS}^2} \tag{7}$$

The k_{opt} form Equation (7) is used to design the optimal number of clusters in the network on every round as used [40]. The k_{opt} depends on the total number of nodes (N) deployed in the region of area $A = M \times M$ square meters, in which the nodes amplify the data and trans-receive with respect to the distance of the base station (d_{BS}^2) and the values are distributed in [46].

F. OPTIMAL NUMBER OF ADVANCED NODES

The entire network setup is assumed to be N sensor nodes deployed in a squared area $A = M \times M$ region. Though sensor nodes are designed with energy heterogeneity, they are all able to sense and transmit data directly to the BS located in the center of the sensor nodes deployed in area A. The total number of nodes N is very optimally divided into two categories (i) Advanced Nodes and (ii) Normal Nodes. Let us assume that μ is the fraction of advanced nodes from the total deployed nodes and $(1-\mu) \times N$ is the normal node count in the deployed area. We assume that all the nodes are deployed randomly and evenly distributed in the RoI. The Advanced nodes have $(1+\eta)$ times higher energy than the normal nodes. The counts of the advanced and normal nodes are estimated from Equations (8) and (9) [47].

$$N_{AD} = \mu \times N \tag{8}$$
$$N_{NOR} = (1-\mu) \times N \tag{9}$$

The fraction of the advanced nodes (μ) allocation is based on the optimal number of clusters k_{opt} and the total number of nodes to be deployed. The value of μ has to be set either equal to k_{opt}/N or greater than k_{opt}/N, which is given in equation (10).

$$\mu \geq \frac{k_{opt}}{N} \tag{10}$$

G. ENERGY ALLOCATION OF NODES

According to the value of μ, the total number of advanced nodes and the normal nodes ratio vary. As the advanced nodes differ from the normal nodes only in the energy capacity of the battery, the Total Initial Energy of the normal nodes E_{T-NOR} and the advanced nodes E_{T-AD} are given in the equations (13)-(16) where the E_0 is the initial energy of the normal nodes and the initial energy of an advanced node in equation (11) and (12).

$$E_{NOR} = E_0 \tag{11}$$
$$E_{AD} = E_0 \times (1+\eta) \tag{12}$$
$$E_{T-AD} = E_0 \times (1+\eta)\mu \times N \tag{13}$$

Can also be rewritten as

$$E_{T-AD} = E_0 \times (1+\eta) \times N_{AD} \tag{14}$$
$$E_{NOR} = E_0 \times (1-\mu) \times N \tag{15}$$

Can also be rewritten as

$$E_{T-NOR} = E_0 \times N_{NOR} \tag{16}$$

Then the total Energy (E_{total}) of the network is certainly probable as in equations (17)-(20).

$$E_{total} = E_{T-AD} + E_{T-NOR} \tag{17}$$
$$E_{total} = [E_0 \times (1+\eta) \times N_{AD}] + [E_0 \times (1-\mu) \times N] \tag{18}$$
$$E_{total} = [E_0 \times (1+\eta) \times N_{AD}] + [E_0 \times N_{NOR}] \tag{19}$$
$$E_{total} = E_0[(1+\eta) \times N_{AD} + N_{NOR}] \tag{20}$$

IV. PROPOSED SYSTEM

This paper focuses on enhancing the energy efficiency of IoT-based Heterogeneous Wireless Sensor Networks to improve network lifetime. The proposed system consists of two phases: Phase I, the Setup state, which involves deployment strategy, clustering, cluster head selection, and finding the energy-optimal routing. Phase II, the steady state, is dedicated to data transmission.

The proposed model setup state is illustrated in Figure 4 and which offers several benefits. Firstly, the proposed model extends the overall network lifetime of IoT-based Heterogeneous Wireless Sensor Networks by improving energy efficiency. This enhancement is achieved through optimized deployment strategies, efficient clustering, and selection of energy-efficient cluster heads. Secondly, the model ensures energy-optimal routing, further reducing energy consumption and prolonging network operation. Additionally, the two-phase approach of the model, separating setup and steady-state operations, enhances the network's overall stability and performance, leading to more reliable data transmission.

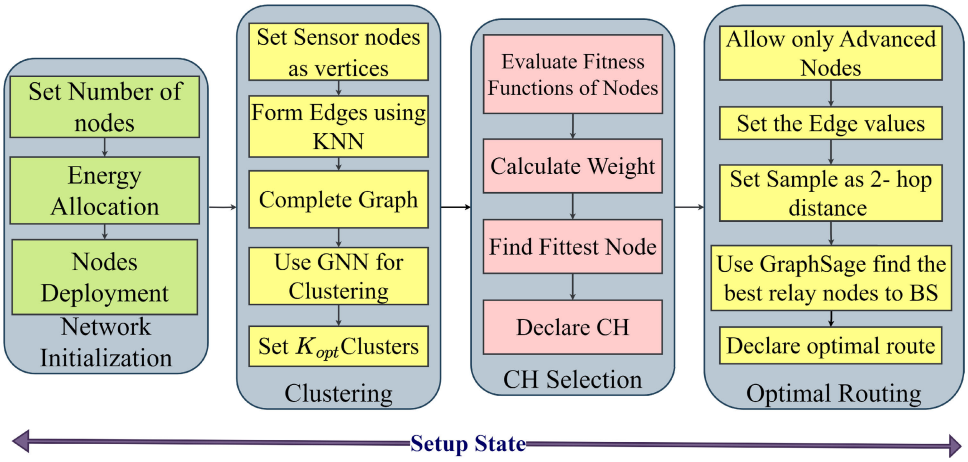

FIGURE 4. Proposed model setup state.

A. PHASE I: SETUP STATE

1) DEPLOYMENT STRATEGY

In a large area network, a square meter area can be divided into multiple clusters of sensor networks. The sensor nodes are deployed in the region to cover the area to gather information about the environment. The proposed model has energy- heterogeneous nodes, hence the nodes are deployed in a different strategy. As the normal nodes are higher number of advanced nodes, they N_{NOR} are deployed randomly. The number of advanced nodes (N_{AD}) is estimated as per equation (7) to set the μ and the μ fraction of advanced nodes are deployed uniformly in the RoI as shown in Figure 2. The significance of combining random and uniform deployment strategies lies in achieving a balanced and effective coverage of the area. Random deployment ensures that normal nodes are spread across the region, providing a basic level of coverage. Meanwhile, uniform deployment of advanced nodes within the RoI ensures a low probability of coverage holes, which enhances the overall performance and efficiency of the network.

2) CLUSTER FORMATION

Graph Neural Networks (GNNs) offer a substantial advancement over traditional clustering models in Wireless Sensor Networks (WSNs), providing improved performance, scalability, and adaptability. In the GNN model $\mathbb{G} = (\mathbb{V}, \mathbb{E})$, where the nodes are represented as vertices ($\mathbb{V}$) and the connections between them as edges ($\mathbb{E}$). The edges are established by determining the distance between a node and its neighbours using the K-nearest neighbour (KNN) method [48], [49], where K is set to 1 to ensure that each node has at-least one edge to a neighbour node. These edges are directional, pointing towards the closest neighbour ($\mathbb{E} = (v, u)|v, u \in \mathbb{V}$).

To avoid the potential issue of multiple subgraphs in the network and ensure a complete graph structure, the K is incremented by 1 until the graph has complete edges between subgraphs. KNN creates a complete graph based on the edge weights of the neighbours. KNN algorithm iteratively adds the edges of the neighbours and selects the edge with the smallest weight that connects a vertex. This process continues until all vertices are included in the tree, resulting in a connected acyclic subgraph with a minimum possible total edge weight.

The KNN approach guarantees that all nodes in the network are interconnected,thereby preventing the isolation of nodes and enhancing the overall graphical connectivity of the network. Additionally, weights ($\omega_e(i, j)$) are assigned to the edges based on the location (x,y) distance between nodes (i, j), calculated using the Euclidean distance as in equation (33) by setting $d = 2$. Nodes are characterized by spatial layout features and self-accessed features ($\mathbb{F} = f_1, f_2, \ldots, f_n$), that is including node id, node location (x, y), distance from BS, residual energy, and the total number of connected least neighbour node edges as shown in Figure 5.

Each node in the network has its member neighbouring nodes represented as (m_v). The objective of the clustering stage is to estimate the number of optimal clusters and group the nodes in the clusters, where the total number of optimal clusters is estimated from equation (7) and node (v) with its neighbour (u) is grouped by GNN. To convert the objective of estimating the optimal number of clusters and grouping nodes into the optimal number of clusters in the formula for the objective function, we can combine the two objectives into a single formulation function. The optimal number of clusters is denoted by K_{opt} and the grouping of nodes into clusters is represented by $c(u, v)$ where v is the node with the highest edges, and u is the neighbouring node that becomes a member node of the cluster from the neighbouring node set N_v. The formulated objective function is given in equation (21).

$$minimize K_{opt}, c(\cdot) : [\{m_v + \textstyle\sum_{u \in N_v} c_{(u,v)} | v \in \mathbb{V}\}] \quad (21)$$

The objective function is achieved using the GNN, which learns from the node representation. In node representation

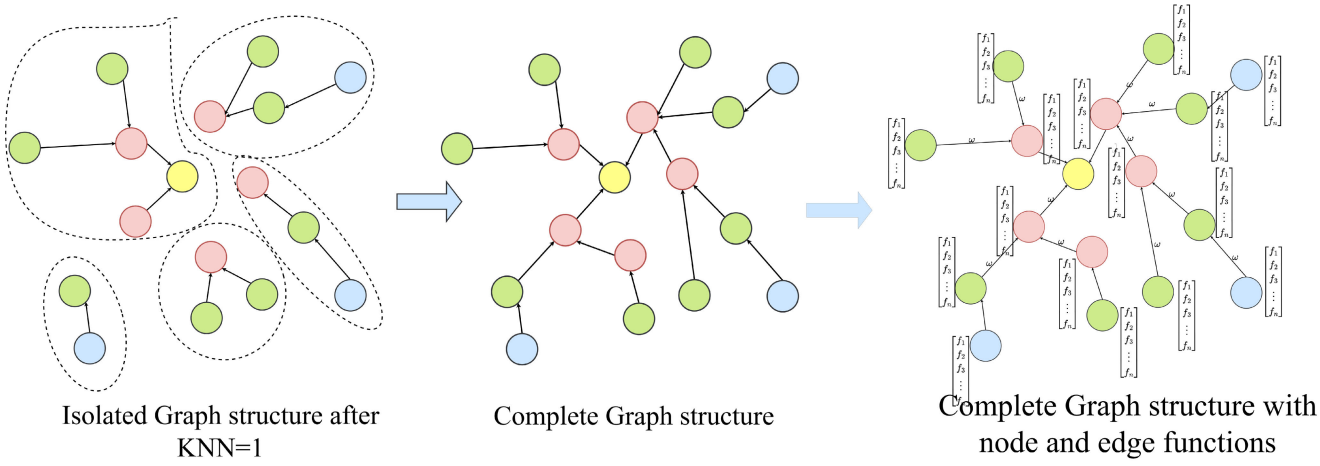

FIGURE 5. Initial graph network formation.

learning, the node features and the edge values are learned by the GNN model from the graph topology as an adjacency matrix ($A_m \in \mathbb{R}^{V\times V}$) where V is the number of nodes in the network. The Input features and edge metrics of every node in the network are passed to the neighbours to understand the relationship between the nodes that are constructed in a feature matrix as $\mathbb{F} \in \mathbb{R}^{V\times n}$, where n is the number of node features. The GNN has the concept of a message passing neural network (MPNN), which comprises three stages such as messaging passing, aggregating and updating to learn the node and edge states by staking the information in a fixed size vector in the encoding stage. In the message-passing stage, each node sends its hidden state h_n^l to its neighbour nodes, which denotes the hidden state of n^{th} node in l layer. The network is initialized as $h_v^0 = \mathbb{F}_v$, where the $\mathbb{F}_v$ is the feature vector of node v. The hidden function of every stage is generated as in equation (22) and forwarded to the neighbouring nodes as in equation (23).

$$h_v^l = \sigma(\omega_l \sum \frac{h_u^{l-1}}{|\mathbb{N}_v|} + b_l h_v^l - 1) \tag{22}$$

Equation (22) comprises two units with a non-linear activation function (σ), where the first unit is the averaging of hidden values from the set of all the neighbouring nodes of node v with weight (ω),and the second unit is the bias (b) multiplied by the previous layer embedding of node v.

$$Message(m_{v,u}^l) \leftarrow msg(h_v^{l-1}, h_u^{l-1}), \forall(u, v) \in \mathbb{E} \tag{23}$$

$$Aggregate(agg_v^l) \leftarrow agg(m_{v,u}^l | u \in \mathbb{N}_v, \forall u \in \mathbb{V}) \tag{24}$$

$$Updateh_v^l \leftarrow updt(h_v^{l-1}, agg_v^l), \forall v \in \mathbb{V}. \tag{25}$$

In the aggregation stage, all the nodes receive messages passed from their neighbours ($m_{v,u}^l$). In aggregation, the messages of neighbouring nodes are summed or averaged (agg_v^l) in equation (24). In the proposed model, aggregation is used as the mean function given in equation (25) where agg is the mean of the weighted average of neighbours as in Equation (27).

$$h_v^l = \sigma([\omega_l \cdot agg(h_u^{(l-1)}, \forall u \in \mathbb{N}_v), b_l h_v^{l-1}]) \tag{26}$$

$$agg = \sum_{u\in\mathbb{N}_v} \frac{h_u^{(l-1)}}{|\mathbb{N}_v|} \tag{27}$$

The update stage performs the message update with its neighbouring node information h_v^l as in equation (26). After updating of all node details, the GNN is trained for the iterations, and the loss function is used to refine the values by backpropagation. The loss function is precisely structured for efficient clustering by incorporating intracluster similarity and intercluster dissimilarity, where the intracluster similarity term must be maximized and the intercluster similarity must be minimized. Hence the Silhouette Coefficient, which comprises intercluster similarity and intracluster dissimilarity, is calculated for every node. The Silhouette Coefficient is used to measure the quality of a cluster by accessing the distance from two nodes $d(x_i, x_j)$, where the clusters are denoted as C_k and $\{k = 1, 2, 3, \ldots, k_{opt}\}$ of the nodes $X = \{x_1, x_2, \ldots, x_N\}$. Initially the intracluster similarity is evaluated for node x_i with all other intracluster nodes x_j in cluster C_i as given in equation (28).

$$a(x_i) = \frac{1}{|C_i| - 1} \sum_{x_j\in C_i, i\neq j} d(x_i, x_j), \tag{28}$$

where the low value of $a(x_i)$ represents high similarity within the cluster and a high value of $a(x_i)$ represents dissimilarity of the node within the cluster. The minimum average of the intercluster value of the node (x_i) is estimated with all the other nodes x_j cluster-wise as in equation (29), where the high values of $b(x_i)$ indicate that the node is different from the other cluster and a lower value indicates the closeness of the node to the cluster.

$$b(x_i) = \min_{j\neq i} \frac{1}{|C_i|} \sum_{x_j\in C_j} d(x_i, x_j), \tag{29}$$

The silhouette score (S_c) of node x_i must be the minimum of $a(x_i)$ and maximum of $b(x_i)$, and is expressed as in equation (30).

$$S_c(x_i) = \frac{b(x_i) - a(x_i)}{max\{a(x_i), b(x_i)\}} \tag{30}$$

The silhouette score must be the maximum to obtain a good quality cluster hence, the clustering loss is framed as in equation (31).

$$L_c = 1 - S_c(x_i) \tag{31}$$

The decoder layer is used to extract the final values of the edges used to cluster the nodes. The decoder computes the inner product of the hidden states of the nodes at both ends. This inner product serves as a scalar value assigned to the edge, representing the relationship or similarity between the nodes connected by the edge. Finally, the clusters are formed, and the entire proposed model of clustering is structured in figure 6. The proposed model of KGNNs can exploit the complex relationships between nodes based on their spatial layout, connectivity patterns, and other features. This allows GNNs to create more precise and context-aware clusters, leading to a more efficient use of resources and better overall network performance.

3) CLUSTER HEAD SELECTION

Fitness-based cluster head selection is evaluated by considering highly impacted elementary parameters to generate the fitness factor of a node with AHP weights to be elected as a cluster head in this phase. AHP excels in environments where different criteria need to be prioritized. In CH selection, factors such as residual energy, distance to the base station, intra-cluster distance, and communication cost are critical. AHP enables to assign weights to these factors based on their relative importance to network performance, which integrates with the heterogeneous nature of WSNs. Additionally, AHP allows fine-tuning of weights based on network-specific priorities, which varies with application requirements. In the proposed model, a network focused on energy efficiency, hence the AHP assigns higher weights to residual energy and prioritize distance to the base station. This adaptability makes AHP suitable for diverse scenarios and scalable as network priorities shift over time. The proposed model structured approach in maintaining a balanced CH selection process by confirming that all the fitness functions are consistently evaluated to reduce subjective bias in weight assignments.The primary eligibility of the node to participate in the election is that it must be an alive node whose residual energy must be greater than the eligible node energy, calculated as in equation (32).

$$E_{NE} = \frac{ResidualEnergyofNode(E_{RE(CH)})}{E_{CH-TOT)}} \tag{32}$$

The focus of the paper is not only on weight estimation but also on decreasing the complexity of analysis by implementing priority-based AHP which balances the weightage distribution on ranking. The fitness functions for evaluating the fitness value are as follows.

1) Distance from node to the Base Station: As nodes forward their position (x, y) to the base station, the distance is calculated by using the Minkowski distance given in equation (33). The Minkowski distance is formulated by two different prominent formulas of the Euclidean distance and Manhattan distance. The simplest rule by changing the d value $= 2$, this equation acts as the Euclidean distance, and while setting the $d = 1$, the formulae turn into Manhattan distance. From the study of the best formulation on the dependent variable, it is found that the node deployment is random, and the Euclidean distance formulae are efficient, however for uniform deployment, Manhattan performs better than Euclidean distance. Therefore on the random deployment set the $d = 2$ and on the uniform deployment set $d = 1$ for proficient distance estimation.

$$D_{N-BS} = \sum((|x_{BS} - x_l|^d + |y_{BS} - y_l|^d))^{\frac{1}{d}} \tag{33}$$

2) Lifetime of a CH: The node lifetime is calculated as the residual energy of the node and the data transmission energy required in Equation (34) to transmit the data to the base station. The node lifetime is the highest priority factor considering the overall network lifetime and performance.

$$CH_l = \frac{ResidualEnergyofCH(E_{RE(CH)})}{TransmissionEnergy(E_{TX(CH-BS)})} \tag{34}$$

3) Average intra-cluster distance: The logic behind the calculation of the intra cluster distance is that, when the node has multiple nearby neighbouring nodes, then the distance of transmission from node to CH is reduced, which defends more energy in every transmission. Therefore the neighbouring nodes are calculated using the average distance from the nodes to the node assessed to become the cluster head.

$$D_{N-CH} = \sum(|x_N - x_{CH}|^d + |y_N - y_{CH}|^d) \tag{35}$$

$$N_N = \frac{1}{C_M} \sum_{l=1}^{C_M} distance(D_{N-CH})_l \tag{36}$$

4) Max Power transmission: The maximum power depletion of a member node from any of the created clusters in the entire network and its peak transmission energy to forward the data to the cluster head are formulated by equation(37).

$$P_{i.max} = max(E_{TX(node(i)-CH)}) \tag{37}$$

5) Average lifetime of the nodes in the cluster: The individual lifetime of the nodes is calculated by the resemblance of equation (38) for finding the node lifetime and that is used to find the average lifetime

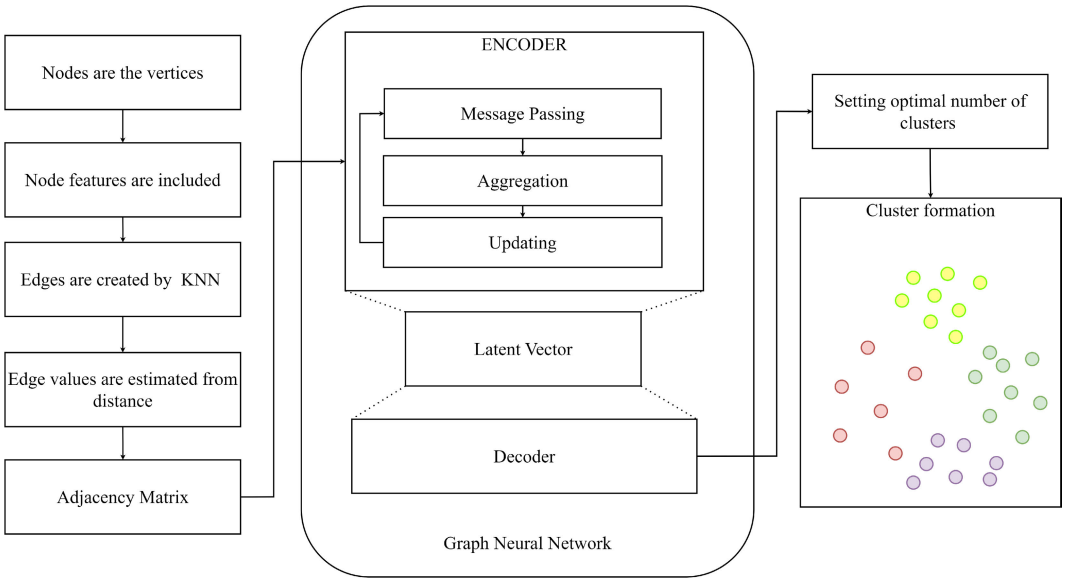

FIGURE 6. Initial cluster formation.

of the nodes in a cluster. This is taken as the average lifetime of the cluster.

$$L_N = \frac{E_{RE}}{E_{TX(node(i)-CH)}} \tag{38}$$

$$L_{avgMN(cluster)} = \frac{1}{C_M}\sum_{l=1}^{C_M} L_N \tag{39}$$

4) WEIGHTS

As this paper proposes that the cluster head selection depends on the weights, the basic summation of weights (ω_i) assigned to find the fitness function (f_v) must be equal to one. As we are using five different fitness values,we used

$$\sum_{i=1}^{n} \omega_i = 1 \tag{40}$$

$$\omega_1 + \omega_2 + \omega_3 + \omega_4 + \omega_5 = 1 \tag{41}$$

5) FITNESS VALUE

The fitness function for the nodes to become a cluster head is formulated with the foremost priorities for energy and distance. This paper proposes a detailed hierarchy for weighting the nodes on the above-mentioned five factors by scalarizing functions bound to the algorithm. The hierarchical arrangements of weighing stages are introduced in the process of the fitness function by initially grouping the nodes, relating the entities, setting up the priority factor, and assigning weights to the nodes assumed to be the cluster head.

$$f_v = \omega_1 A + \omega_2 B + \omega_3 C + \omega_4 D + \omega_5 E \tag{42}$$

As cluster head selection is an exceedingly convoluted task in the computational, link, and energy heterogeneity of WSN, an efficient model must be introduced in various fields of heterogeneous networks. In a network of computational heterogeneity, the node's processing power, and memory are considered as weighing factors. In a link heterogeneous network, the link of asymmetric radio transmission power for the minimum path range length, speed of mobile nodes, the distance from the cluster head to the base station using the Euclidean distance and link of the converse path is considered for weighing the nodes. In an Energy heterogeneous network, the lifetime of the cluster head and the average lifetime of cluster member nodes in a cluster are considered weighing the fitness factors. These entities lead to a more complex or non-optimized solution in the process of weighting the impeccable cluster head. In the Proposed model, the fitness value is the summation of all five fitness functions, but the fitness functions are a combination of the Min and Max terms with normalized values. Hence, to make it equal, the reciprocal of a few fitness functions is used, as given in Equation (43).

$$f_v = \omega_1\left(\frac{1}{D_{N-CH}}\right) + \omega_2(CH_l) + \omega_3(L_{avgMN(cluster)}) + \omega_4\left(\frac{1}{P_{i.max}}\right) + \omega_5(N_N) \tag{43}$$

Hence, we have proposed a modest form of weighing process that takes the highly essential entities for weighing the nodes to bring out the least ranked node as a cluster head in a cluster by using AHP. The entities are introduced by representatives A, B, C, D, and E. These five entities are broadly classified under only two categories of consideration: (i) distance among the nodes and to the base station, and (ii) average energy of the cluster and its inter-cluster nodes. In these two categories, weights are assigned to the priorities of the entity. Primarily, the priority is given to proximity entities because, according to equation, the distance is directly proportional to the energy consumption of a node while transmitting and receiving a bit of a data

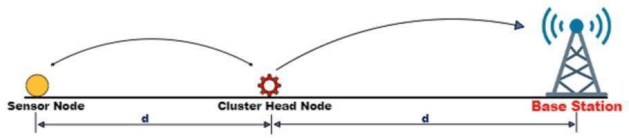

FIGURE 7. Data transmission through CH.

TABLE 3. Priority rank.

Priority	1	2	3	4	5
Fitness factor	A	D	E	B	C

packet. In a clustered network, the direct transmission and reception distance is alienated by half if it's a two-hop data transmission, but the relay of data can be sectored further in multi-hop transmission. The energy required to transmit the data directly to the BS from its location is reduced by forwarding it to the CH which is located between the nodes and the BS. Figure 6 shows how the distance of transmission is further reduced by the multihopping technique. Hence, the proximity of the node to the cluster head and to the base station is a highly prioritized entity in the weighing factor. Thus, the distance between a node and its CH is considered to be (A, E). The distance of the BS versus the nodes to be a CH is assessed by the equation DN_{BS} represented as A, for simplicity in further processing.

The *Node distance from the base station* (A) is set as the foremost factor in the fitness function, therefore it is considered as the first fitness factor for weighing. The remaining three energy-dependent fitness factors are, the *Lifetime of the node assessed to become a cluster head* is designated as D, the Lifetime of member nodes is taken in the summed average that will be represented by C, the *peak power consumed* by any of the nodes in a cluster is designated by B, and the *intra-cluster distance* is represented by (E), which are evaluated by equations (32)-(38).

Although the values are obtained by equations, these fitness factors must be set to assign weights. As A is set in first place in order, the remaining entities are set into a series of highly prioritized factors (D) lifetime of a cluster head node of the node is chosen to be the head among the energy-related entities that will be followed by the maximum neighbouring node entity E and the last two entities (B) peak power consumption proceeds with the average lifetime of member nodes (C). The ranking order is given in Table 1.

Table 1 lists the basic energy factors B, C, D, and E. These four factors can be ranked in twenty-four possible orders in combination. Because the weighing process depends on the preceding entity for calculation, finding the optimal order is the objective of embedding the fitness function on the cluster head.

In the process of finding the best order of entities, the study of homogeneous and heterogeneous network protocols is considered and simulated to find the optimal combinations. The above combinations are simulations with various initial

TABLE 4. Point ranking table.

Fitness functions	A	D	E	B	C
Points Rank	10	9	8	7	6

energy values and the results indicate that the higher energy-consuming nodes will drain their energy earlier. Hence, the node with higher energy consumption is weak for the race to become a cluster head. The next priority is given by the inference that the higher residual energy nodes have greater possibilities to becoming a cluster head and can also withstand a longer duration of its responsibilities. Finally, it is inferred that a cluster with higher average energy may lead to an enhanced network lifetime. As we have considered the same parameters henceforth, we have followed the same order of ranking, but the highest neighbouring node factor is also taken into consideration in our proposed model. For that, the nodes with the highest neighbour must be given priority because if the nearest neighbours are more, then the data transmission range of those nodes will be reduced which will influence the reduction of energy consumed by the nodes to communicate the data. Therefore, we obtained the rank order as mentioned in Table 1.

a: POINTS RANK

The establishment of the ranked entity is followed by a weighing process to obtain the fitness function. Step 1 associates the near-ranked entities and points are given by comparing their priority at the base station with a score of 10 points, and that with a lower priority, is given a lower relative score.

Let's assume that the point rank possessed by the base station is listed in Table 2.

b: RELATIVE POINTS

The Relative Points (P_R) are generated from the five factors, and we obtained four results of comparison and the non-comparable entities are not considered (not applicable) as shown in Table 3.

When two factors are paired and compared, the preference value should satisfy the reciprocal condition. For instance, if A is x times as important as B, B is $\frac{1}{x}$ times as important as A, and vice versa. The points are given initially to the higher ranker's ($T_{high-rank}$) by the normalized value 10 and the relative of the next lower ranker entity ($T_{low-rank}$) is given under consideration with respect to the normalized value as in equation (44).

$$P_R = P(A) = \frac{T_{low-rank}}{T_{high-rank}} * 10 \tag{44}$$

For example, Table 3 is filled by the relative ranking by comparing entities A with D, and the relative importance value of A is $T_{high-rank} = 10$, which is normalized by the highest normalizing point P(A) = 10. The relative importance value of D is considered as low ($T_{low-rank}$), so the points for

TABLE 5. Relative points table.

Comparison	P(A)	P(D)	P(E)	P(B)	P(C)
A WITH D	10	9	Not applicable	Not applicable	Not applicable
D WITH E	Not applicable	10	8	Not applicable	Not applicable
E WITH B	Not applicable	Not applicable	10	7	Not applicable
B WITH C	Not applicable	Not applicable	Not applicable	10	6

P(D) are calculated as in equation (45).

$$P(D) = \frac{T_{\text{low-rank}}}{T_{\text{high-rank}}} * (\text{Prior entity value}) = \left(\frac{9}{10}\right) * 10 = 9. \quad (45)$$

As the remaining entities are not directly related to A and D, we mentioned them as not applicable. The next comparison is between D and E, where E has a low rank, therefore we get $P(E) = (8/10) * 9 = 7.2$. The remaining entities are compared and are listed in Table 4 for reference.

c: POINT BINDING VALUE

The point binding value (P_{bv}) method is used to decrease abnormalities in computed values as well as anomalies in the weighing process using the linear interpolation method. This is done to bind the best window of difference between the fitness factor's maximum and lowest point ratios i.e., P(A)-P(C). A larger difference value leads to higher reliance on specific factors and the lower difference degrades the order of priority, which is imposed on the main objective of an energy-efficient network. The higher reliance on a specific factor above 20 percent of variance steers the results of the protocol into unpredictability and a variance lower than 20 percent diminishes the priority factor. Accordingly, the lowest point ratio is smoothened by 20 percent by incrementing the point ratio value of the least ranker to reduce the difference range between the highest and least rank point ratios. Therefore, the least relative point ratio of value 3.024 is enhanced and the new bounded least point is 4. It is important note that the least binding value is dependent on the required disparity between the weights. When the least relative point ratio is very low, the binding value can be chosen to be higher and all relative points are linearly interpolated.

To formulate this, we have stated that $P_{bv(x)}$ is the point binding value, (P_{int}) point interval, (P_{lr}) least point ratio i.e.,3.024, Current Point Ratio (P_i), Initial Point Range (V_i), and Bounded Point Range (V_b).

$$P_{int} = \left(\frac{P_i - P_{lr}}{V_i}\right) * V_b \quad (46)$$

$$P_{bv} = P_{int} + (P_{blr}) \quad (47)$$

The highest point ratio is 10, and the initial point range is taken from the different values of the highest and lowest points, i.e., $V_i = (10 - 3.024) = 6.976$. The Bounded Point Range (V_b) is the difference value of the highest P_R and the new least binding point (P_{blr} i.e., 4) as in equation (48).

$$V_b = P_R - P_{blr} = (10 - 4) = 6. \quad (48)$$

Calculations:

$$P_{int}(D) = \frac{9 - 3.024}{6.976} * 6$$
$$P_{int}(D) = \frac{5.976}{6.976} * 6$$
$$P_{int}(D) = 0.857 * 6$$
$$P_{int}(D) = 5.14$$

Where

$$P_{br}(D) = P_{int}(D) + P_{blr}$$

Therefore

$$P_{br}(D) = 5.13 + 4$$
$$P_{br}(D) = 9.14$$

To find the point binding value of D, initially, the P_{int} is calculated by the interval from point D ratio ($P_{int} = 9$) to the least relative point and the lowest point interval is 5.976 from the lowest end. The new P_{int} (D) = [((5.976)/6.976)* 6] = 5.14, and the interval of P_{int} (D) is enhanced to the new scale binding value, that is P_{bv} (D) = 5.14 + 4 = 9.14. Similarly, the intervals from E to C and B to C are computed and are shown in Table 4.

d: WEIGHING

The sum of point binding values ($P_{bv(x)}$) given in Table 4 is taken i.e., 36.43 and the point bounded value of the fitness entities is divided by that. We acquired the weights as given in Table 5 and the summation of weights is equal to 1.

After finding the weights as in Table 5 of every fitness factor, which is applied in equation (43), the fitness values are estimated. The estimated value is arranged in descending order, and the node with the highest value is ranked the least and selected as the cluster head in the round.

6) RELAY NODE SELECTION FOR THE OPTIMAL ROUTE

GraphSAGE (Graph Sample and Aggregation) is also a GNN technique that learns node representations by sampling and aggregating information from a node's local neighbourhood. This addresses the challenge of scalability in GNNs by operating on large graphs efficiently. GraphSAGE operates in multiple layers, where each layer samples a fixed number

TABLE 6. Weight table.

	A	D	E	B	C
Relative Points (P_R)	10	9	7.2	5.04	3.024
Point binding value	10	9.13	7.6	5.7	4
Weights	$\omega_1 = 0.27$	$\omega_4 = 0.25$	$\omega_5 = 0.21$	$\omega_1 = 0.16$	$\omega_3 = 0.11$

TABLE 7. Final weight table.

P_{bv}	10	9.13	7.6	5.7	4
Weight ω_n	ω_1 $= (10/36.43)$ $= 0.27$	ω_4 $= (9.13/36.43)$ $= 0.25$	ω_5 $= (7.6/36.43)$ $= 0.21$	ω_2 $= (5.7/36.43)$ $= 0.16$	ω_3 $= (4/36.43)$ $= 0.11$

of neighbours for each node and aggregates their feature information to update the node's representation. This process allows GraphSAGE to learn embedding for nodes in a graph by capturing both local and global graph structures [50].

In the proposed model, GraphSAGE is utilized for finding the optimal relay nodes and the routing is followed as in [51]. The process begins with the farthest CH from the BS, where a set of relay nodes is selected to establish a connection between the CH and the BS. GraphSage learns node representations by sampling and aggregating information from a node's local neighbourhood, which incorporate as an efficient model for routing decisions in WSNs. It efficiently identifies suitable relay nodes by considering the node features and neighbourhood information, thereby optimizing data transmission and minimizing packet loss. Through its ability to learn from the network structure and node attributes, GraphSage enables effective routing decisions to optimize the energy efficiency in the network. GraphSage incorporates only the advanced nodes deployed uniformly across the region of interest exclusively participate in relay node selection, thereby reducing the excess workload on normal nodes. GraphSage is employed to determine the optimal relay nodes for data transmission and path setting. In this model, the sample range is fixed to the 2-hop distance nodes from each node using the KNN algorithm, with *Meanagg* utilized for aggregation as in equation (27) and Figure 8.

GraphSage reduces latency in routing decisions (Sr) by considering only nodes within a 2-hop neighbourhood. The Nodes (AD) in the 2-hop distance of the CH forward the message of the hidden state comprising the features of node location (x, y), residual energy of the node, distance from BS, distance between the nodes, Packet Reception ratio (PRR), and load of the node.

The load of node ($Load_r$) is the cumulative traffic load of r, which is actually the sum of packets generated by the node at the current round (r_p) and the packets travel through (r_{pr}) node r from neighbouring nodes (u) in order to reach the sink node, and it is represented by expression (49).

$$Load_r = r_p + \sum_u r_{pr} \tag{49}$$

Nodes can quickly identify suitable relay nodes without needing to search the entire network topology, leading to faster data transmission. Traditional GNNs may involve aggregating information from distant nodes, leading to increased computational overheads and communication costs. Therefore in GraphSage, the aggregation process focuses on nearby nodes within 2-hop distance which reduces overhead and improves the network efficiency. GraphSage helps find the closest neighbouring node between the BS and the CH. For distant CHs, a middle node is selected to transmit data to the BS. To ensure efficient relay node selection, criteria such as proximity to the CH, avoidance of multiple hops, and adherence to the maximum transmission path distance are considered. This problem is solved by examining only the advanced nodes with four basic constraints:

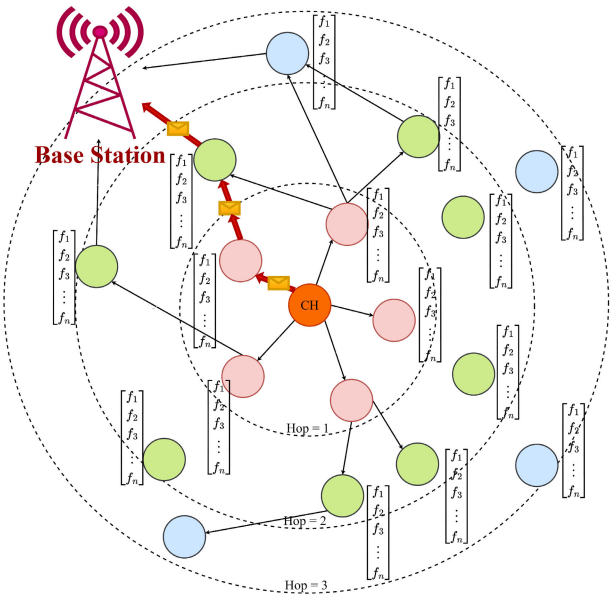

FIGURE 8. Routing in the network.

- The selected relay node from the CHs must be capable of forwarding its data as well as the data transmitted from the other nodes (M_v).

$$\forall r \in R \tag{50}$$

where, r is a node capable of forwarding data from other CH and M_v R is set of relay nodes selected.

- The CH node selected as the relay node cannot be the relay node for another CH.

$$\forall i, j \text{ where } i \neq j, \forall r \in R_i, CH_j \notin R_i \tag{51}$$

  where all relay nodes (r) from the set of relay nodes (R_i) for CH_i cannot be relay nodes of CH_j.
- The total energy of passing data must not be much greater than the current node transmission path (tx) energy in distance to the CH and BS.
- If the last condition is not satisfied, the node can directly transmit data to the BS.

The eligible relay nodes as the next hop is determined based on both the energy cost and the distance involved in data transmission. Relay nodes are chosen to ensure minimal energy consumption as in equation (52) and also maintaining an optimal transmission distance as in equation (53), thereby balancing energy efficiency and reliable data delivery within the network.

$$\Delta E = E_{\text{CH,BS}} - \left(E_{\text{CH,Relay1}} + \sum_{i=1}^{n-1} E_{\text{Relay}_i,\text{Relay}_{i+1}} + E_{\text{Relay}_n,\text{BS}} \right) \tag{52}$$

$$E_{\text{CH,BS}} = k \cdot D_{CH,BS}^{\alpha} \tag{53}$$

where k is a proportionality constant related to the data packet size and the energy dissipation model, α is the path-loss exponent as in equation (1), $E_{\text{CH,BS}}$ is the energy required for direct transmission from CH to BS, $E_{\text{CH,Relay1}}$ is the energy required to transmit data from CH to the first hop relay node.

$$\sum_{i=1}^{n-1} E_{relay_i,relay_{i+1}} = \sum_{i=1}^{n-1} k \cdot D_{relay_i,relay_{i+1}}^{\alpha} \tag{54}$$

where $\sum_{i=1}^{n-1} E_{relay_i,relay_{i+1}}$ is the total energy consumed by transmissions between consecutive relay nodes and $E_{\text{Relay}_n,\text{BS}}$ is the energy required to transmit data from the last relay to the BS.

To compare the distance between the Cluster Head (CH) and the Base Station (BS) ($D(CH, BS)$) with the total distance traversed through relay nodes, we consider the combined distances of all individual segments in the relay-based path from the equation (33). This includes the distance from the CH to the first hop relay node ($D_{(CH,Relay1)}$), the cumulative distance between consecutive relay nodes ($\sum_{i=1}^{n-1} D_{\text{Relay}_i,\text{Relay}_{i+1}}$), and the distance from the last relay node to the BS ($D_{\text{Relay}_n,\text{BS}}$). The comparison helps to evaluate whether the relay-based path is more efficient in terms of distance, providing a basis for selecting the optimal route for data transmission. The unnecessary energy consumption and delays can be avoided, ensuring an efficient and reliable communication route in the network by minimizing the total path distance.

B. PHASE II: STEADY STATE

The study state is initiated after the setup state by finding the optimal number of clusters and estimating the fitness values of the nodes to become cluster head, assigning weights to a fitness function, finding the least valued node among the other nodes in the cluster, and declaring it as a CH. This is followed by the estimation of the optimal routing path.

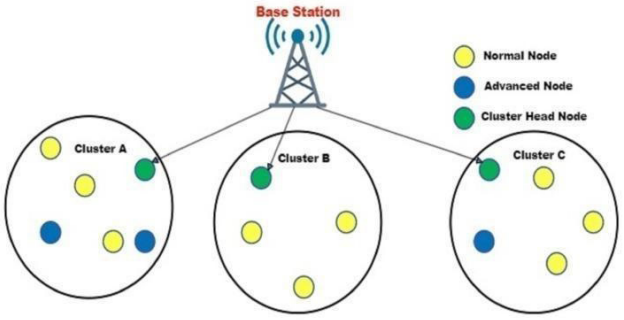

FIGURE 9. Declaration of CH.

Following the declaration of cluster heads (CHs) and the optimal path, nodes forward their sensed data to the CH within allocated TDMA slots. Subsequently, the CH aggregates the data forwarded from the nodes and transmits along the optimal path. The time taken for this single process of transmission is referred to as a round. Upon receiving data from the nodes, the cluster head obtains information regarding the residual energy of each node. When a node's energy level reaches zero, it is designated as a Dead node. The energy quality of the network is determined by the time it takes for the first node to be tagged as dead and the total duration of all node failures. Dead nodes are excluded from further processing within the network.

C. PROPOSED ALGORITHM

The proposed algorithm is divided into two phases. Algorithms 1, 2, and 3 are for initialization, clustering, cluster head selection, and optimal routing, respectively, and Algorithm 4 is for data communication. In the algorithm of data communication, the while loop function is designed to calculate the residual energy of the CH and the member nodes and when the residual energy of the nodes is less than or equal to zero then the node is tagged as dead. If the residual energy is greater than the transmission energy then the node is considered as an alive node for data transmission and reception.

V. DISCUSSION OF SIMULATION AND RESULTS

The proposed algorithm has a distinctive method of cluster formation, calculating the weightage and fitness function to elect the cluster head, and routing using GraphSAGE. The experiments are performed and evaluated using MATLAB R2020.a. and Tensorflow-GNN V 1.0 simulation software. The proposed algorithm is designed to achieve efficient energy optimization in the multi-level of energy in node deployment, therefore the algorithm has run on the simulation software and compared its results with other algorithms to assess the effectiveness of the proposed algorithm.

Algorithm 1 Clustering

INITIALIZATION
Let's set the $N_i = n$
Set Maximum roundsr_{max}
Set the optimal number of clusters k_{opt} as per equation(7)
Set $\mu \geq \frac{k_{opt}}{n}$
Customize the Nodes as in equations (8) and(9)
Distribute the Energy as in equations (11) and (12)
Deploy the nodes in Area $A = M \times M$ with the Location of(x, y)
while $InitialEnergy \geq E_0$ **do**
  if Advanced node **then**
    Uniform deployment
  else if Normal Node **then**
    Random Deployment
  end if
end while
CLUSTERING WITH KGNN
Set Vertices $\leftarrow N_i$
while clustering **do**
  Set $K = 1$ for KNN
  Create Edges
  for $N_i = 1$ to n **do**
    Check existence of subgraphs
    if Subgraph exists **then**
      Increment $K \leftarrow K + 1$
    else if All nodes are connected (Complete graph) **then**
      Stop incrementing K
      Break loop
    end if
  end for
end while
Estimate $\omega_e i, j$ using eq.(33)
Assign Edge values($\omega_e(i)$)
Train the graph $\mathbb{G} = (\mathbb{V}, \mathbb{E})$
Determine K_{opt}
$N_i \in C_j$
Iterate until convergence:
while not converged **do**
  Compute h_v^l and messages $m_{u,v}^l$ them
  Aggregate agg_v^l
  Update h_v^l
  Compute Lc
  if converged **then** stop
  else if backpropagate **then**
  end if
end while

Algorithm 2 Cluster Head Selection

while for every node **do**
  if $E_{RE} \geq E_{NE}$ **then**
    Compute D_{N-CH}, CH_l, $L_{avgMN(cluster)}$, $P_{i.max}$, N_N
    Set weights to the nodes
    Calculate the Fitness value
    Select the least F_v as cluster head
  else if Normal Node **then**
    Set as Member node
  end if
end while

Algorithm 3 Optimal Route Finding With GraphSage

Initialization:
Incorporate GraphSage for routing decisions
Set $Sr \leftarrow 2$
Utilize Mean aggregation ($Meanagg$) in eq (27)
while for every CH node **do**
  Select AD within 2-hop neighbourhood
  if AD within 2-hop **then**
    Compute h_v^l and messages $m_{u,v}^l$ them
    Aggregate agg_v^l
    Update h_v^l
    If AD eligible $\leftarrow$ set as r relay node
  else if
    then$AD \neq r$
  end if
  Ensure tx path Energy as in eq (52)
  if Total tx Energy is $\leq E_{CH,BS}$ **then**
    Set the Path
  else if
    then Direct transmission to BS
  end if
end while

Algorithm 4 Data Communication

while for every node **do**
  Compute the Transmission Energy E_{TX}
  if $E_{RX} > 0$ **then**
    Consider node alive
    if Node is CH **then**
      Compute E_{DA} and E_{RX}
      Acquire residual energy E_{RE}=E_{RE-1}-($E_{TX} + E_{DA} + E_{RX}$)
    else if Member Node **then**
      Acquire residual energy E_{RE}=E_{RE-1}-E_{TX}
    end if
  else if then
    Tag Node 'Dead'
  end if
end while

A. SIMULATION PARAMETERS

The proposed model utilizes a variety of carefully selected hyperparameters to balance learning efficiency and computational demands. The proposed network model is simulated with the below-mentioned parameters in Table 6 and the hyperparameters of the Neural Network setup are given in Table 7.

TABLE 8. Table of network setup parameter.

Parameters	Values
Initial energy of sensor nodes (Eo)	$0.5J$
Heterogeneity node density fraction	μ
Heterogeneity Energy	$E_0(1+\eta)$J
Total Number of Nodes	$N = 100, 200$
Normal nodes	$(1-\mu) * N$
Network Area	A=$M \times M = 100 * 100$
E_{elec}	50n J/bit
Free Space loss(ε_{fs})	10p J/bit/m^2
Multipath loss(ε_{mp})	0.0013pJ/bit/m^4

TABLE 9. Table of neural network hyperparameters.

Hyperparameters	Values
Number of Epoch	20
Units	128
Learning rate	0.00003
Activation function	Relu
message dimention	64
Optimizer	Adam

The number of epochs is set to 20, providing adequate time for the proposed model to learn intricate patterns within the network without overfitting or unnecessarily increasing computation time. However, additional epochs yield minimal improvements as the model has already converged to an optimal solution. In the proposed model 128 units provide a balance between complexity and computational efficiency, facilitating robust learning of the data transmission paths and network dynamics. In contrast, fewer units 64 have a lower capacity to capture complex patterns, while higher numbers, such as 256 or 512, and extend convergence time due to the increased parameter count. The model is tested with varying learning rates (1.0, 0.1, 0.003, and 0.0003). The larger rates of 1.0 and 0.1 proved unstable, and even 0.003 and 0.0003 are too aggressive, leading to oscillation around the optimal solution. The chosen rate of 0.00003 allows gradual convergence, minimizing the risk of overshooting minima. The ReLU activation function effectively handles data non-linearity, essential for learning diverse node characteristics and interactions. A message dimension of 64 enables the GNN to communicate key features between nodes, and the Adam optimizer is selected for its adaptive learning rate and ability to manage sparse gradients efficiently.

B. MODEL VALIDATION

Model validation in evaluating the effectiveness of clustering algorithms, especially, where optimal cluster formation directly impacts energy efficiency and data routing. In this paper, the silhouette coefficient is employed as a key metric to assess the quality of clusters formed by the proposed model. The silhouette coefficient, which ranges from -1 to $+1$, measures how similar each node is to its own cluster compared to other clusters. A higher silhouette score signifies better-defined clusters with high cohesion and clear separation from neighboring clusters, indicating that the clustering approach effectively groups nodes based on their characteristics. The initial clustering quality of the proposed model is given in Figure 10 where the network is deployed with 100 ans 200 nodes. In both scenarios the average silhouette score is above 0.80, in which 100 nodes network the average score is 0.83 and in the 200 nodes network, the score is 0.82. In both the scenarios the proposed model is efficient in clustering.

C. RESULTS AND DISCUSSIONS

The most formidable metrics such as Network lifetime, overall data transmitted from the nodes to the base station, and the average energy of the network are analyzed to systematically determine and assess the potency of the proposed algorithm. The simulation results of the proposed algorithm are compared with SEP [24], HLEACH [16], the Multi-level Heterogeneous clustering (MultiHet) algorithm [52], MOBGWO [36], and EEHCT [28].

The scalability analysis is crucial for evaluating the robustness of models, hence, the paper included an additional analysis to examine the impact of varying sink positions and different network sizes on overall performance as in Table 10. Additionally, the simulation is done in six cases by varying the fractional values of advanced nodes and level of energy to the advanced nodes in the network, follows the established methods detailed in the reference paper SEP [24]. When the $\mu = k_{opt}/n$ and $\eta = 1$ with 100 and 200 nodes in the network to access the scalability and performance of Computational complexity of GNN in small scale and medium scale network while the BS is in the center of RoI (50, 50) and located away from the RoI (150, 200) as in [53]. This scenario level simulation strengthens the transparency and validity of our analysis approach.

Figure 11 and 12 are plotted on the Number of Alive nodes in every round during the process of simulation to find the energy longevity of the 100 and 200 nodes networks. The cluster head selection and the number of cluster formations play an important role in the individual node lifetime. The modified HLeach protocol has the vertiginous fall around the 1300 round of simulation due to the drained energy of normal nodes initially and the network has been run through the advanced nodes which were overcome by the SEP protocol by enhancing the lifetime of normal nodes and equally utilizing and selecting the advanced nodes as cluster heads but the nodes alive are drastically reduced in from 2500 round. The multi-level heterogeneity algorithm has linear sustainability of the alive nodes but the network could not prolong its lifetime due to the random number of selection of cluster heads. The MOBGWO network's first node dead (FND) earlier than the SEP, HLEACH and the proposed model. The EEHCT has stable decline of dead nodes between FND and last node dead/all node dead (AND) but the death of nodes are too early, even there is no significance remark of advanced nodes in the network. The FND in the proposed model is prolonged than the other models due to the algorithm has

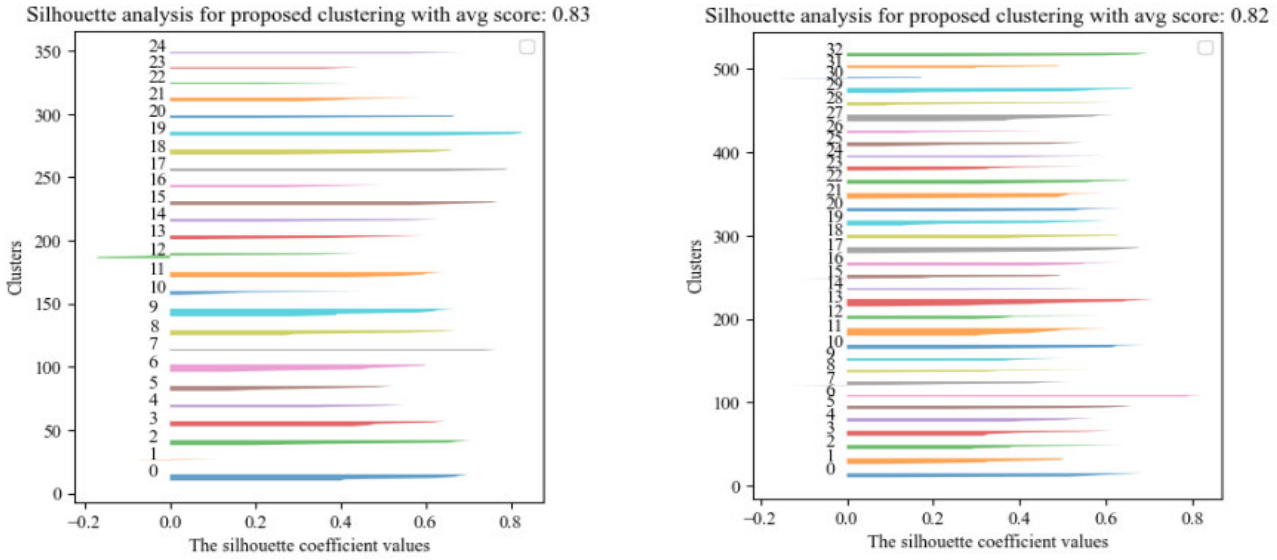

(a) Silhouette score of clusters in 100NN

(b) Silhouette score of clusters in 200NN

FIGURE 10. Average silhouette score of clusters in proposed model.

TABLE 10. Table of simulation scenarios.

	Area	BS Location	No. of Nodes
Scenario 1	100m × 100m	(50, 50)	100, 200
Scenario 2	200m × 200m	(150, 250)	100, 200

the optimal number of clustering methodologies and efficient selection process of fitness value in cluster head election exceedingly reduces the normal node election as cluster head which increases the lifetime of the normal node and also the network lifetime.

To analyse the robustness of the proposed algorithm implemented network Figure 13 and 14 are plotted between the dead nodes in every round of 100 and 200 nodes Network. As per the static quality of the analysis, the study determines the stability of the network by the time the first node is dead. Here the Multilevel heterogeneous algorithm has the first node dead below the round 1000 due to the random selection of the number of cluster heads. When the random selection of the number of cluster heads increases then the normal nodes are forced to be the cluster head which leads to the node dead early. The HLEACH algorithm also follows the random selection of cluster heads with its common threshold probability ratio hence there is not much difference in the round of the FND from the Multi-level heterogeneous algorithm. The SEP has a different threshold probability to select the normal nodes and the advanced nodes but the same as the HLEACH, once the selected node is not given preference to be selected again as cluster head, it leads to the first node dead early. The proposed algorithm gives priority to the Advanced nodes to be elected as cluster heads which gradually reduces the exhaustion of energy in the normal node to be elected as cluster heads. The network's efficiency and performance are quantitatively measured by the data transmitted from the source node to the destination and the rate of data received at the destination node either through single or multiple hops transmission. Hence, Figure 15 is plotted between the packets received at the BS at every round of simulation. Herein, the proposed model outperforms the other models, where the HLEACH has the least data transmission caused by the balanced energy distribution which extends the operational lifespan of the network, allowing it to function for prolonged durations without any node depleting its energy reserves. As a result, the network necessitates fewer packet transmissions, ensuring sustained functionality over an extended timeframe. In SEP, the CH's are elected based on residual energy and proximity to the base station, though this approach can optimize energy efficiency but reduces the packet transmission to the base station. The only consideration of residual energy and proximity may result in some clusters being formed with nodes that have poorer communication links to the base station. Nodes farther away from the base station might experience higher packet loss or lower reception ratios due to increased transmission distances and potential interference. The MultiHet model has moderate data packet reception at BS. The number of data transmitted by the MOBGWO and EEHCT are almost similar. The stability of data transmission is analysed by

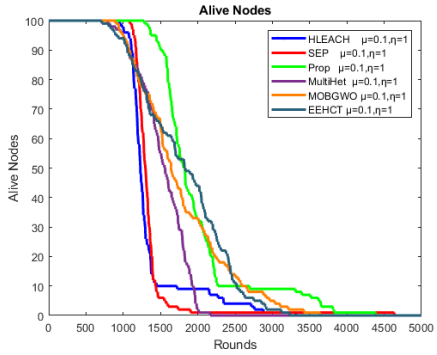

FIGURE 11. Alive Nodes vs Rounds in 100 Nodes network.

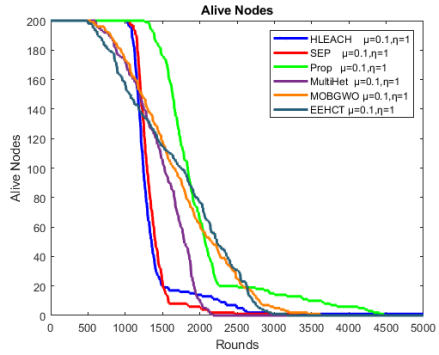

FIGURE 12. Alive Nodes vs Rounds in 200 Nodes network.

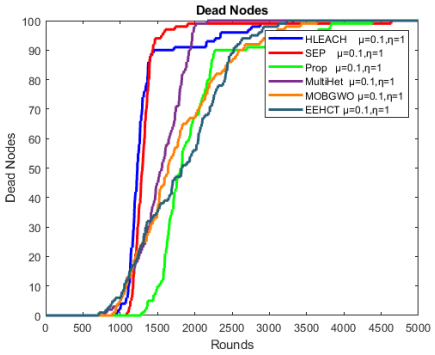

FIGURE 13. Dead Nodes vs Rounds in 100 Nodes network.

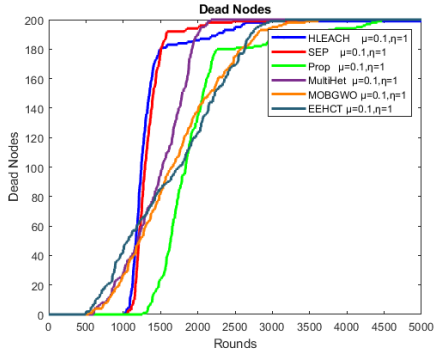

FIGURE 14. Dead Nodes vs Rounds in 200 Nodes network.

figure 15 and 16, where the alive nodes are plotted with the packets transmitted to the basestation of 100 and 200 nodes network. As the nodes dead early in HLEACH and SEP, the networks become partitioned due to nodes dying in a way that disrupts the communication path to the BS, packets from the remaining nodes may not be able to reach the BS. The EEHCT and MOBGWO have higher packet transmission than the HLEACH, SEP and MultiHet but not more than the proposed model.

The extension of the network lifetime has the most significant impact on throughput. Therefore, Figure 17 and 18 depicts the relationship between the number of alive nodes and packets transmitted to the base station in 100 and 200 nodes network. The graph illustrates that as the number of alive nodes increases, there is a corresponding increase in packet transmission. Conversely, when the number of nodes begins to decrease, the throughput also declines. The proposed model demonstrates superior performance compared to other algorithms, particularly in terms of the duration during which all nodes remain operational. Additionally, its effectiveness persists even after the occurrence of the scenario where 90 nodes cease functioning.

The relationship between the average energy of network nodes and the maximum number of rounds is illustrated in Figure 19 and 20, which aid in comprehending the efficient energy utilization of the protocols in 100 and 200 node network. Despite the allocation of Heterogeneous initial energy for normal and advanced nodes, Hleach and SEP demonstrate similar levels of energy depletion due to the probability-based random selection of nodes to serve as CHs. The MultiHet algorithm has a moderate average energy due to the method of functional election of cluster head. The average residual energy of the network the MOBGWO has much higher than the MultiHet but due to optimal CH selection and not higher than the EEHCT. As the proposed model setup state is especially designed for efficient utilization of residual energy using GNN in the clustering and routing, the model outperforms other models in all the scenarios. At some points, the average energy of the EEHCT algorithm is more than the proposed algorithm but it falls immediately in further rounds without the proper stability when the number of nodes is less. It clearly shows that the proposed algorithm has a higher network energy efficiency than other protocols. All the cases of the models are accessed with 100 and 200 nodes in the same network area, to evaluate their scalability and robustness across various network sizes. Algorithms that perform well with a small number of nodes may not necessarily scale effectively to larger networks. By testing with different node numbers can determine if the algorithms maintain their effectiveness, stability, and efficiency across a range of network sizes, ensuring their applicability in real-world scenarios with diverse deployment scales.

1) CASE 1

The case 1 scenario is illustrated with figures, and in tables 11 and 17. Tables 11 and 17 are generated by case 1 for 100 nodes and 200 nodes with $\mu = 0.1$ of advanced nodes

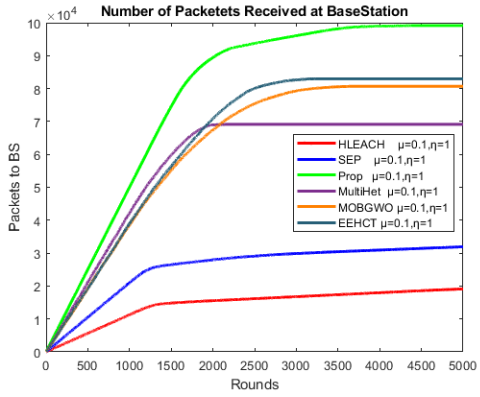

FIGURE 15. Packets to BS vs Rounds in 100 Nodes network.

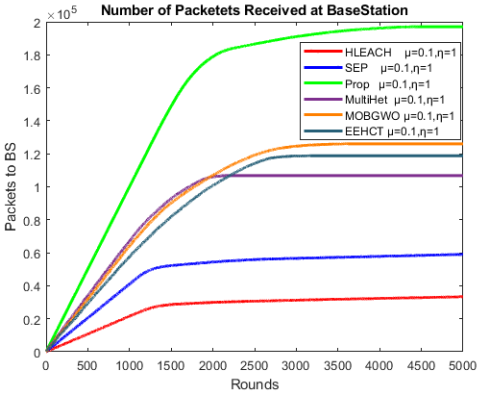

FIGURE 16. Packets to BS vs Rounds in 100 Nodes network.

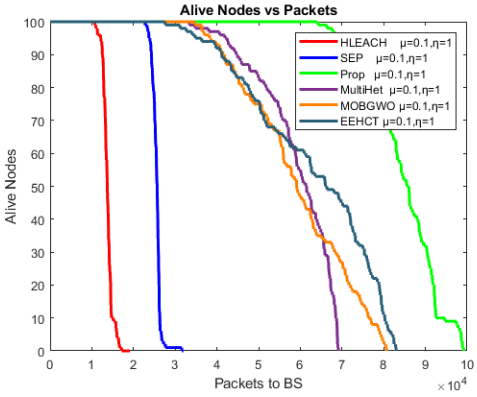

FIGURE 17. Alive Nodes vs Packets to BS in 100 Nodes network.

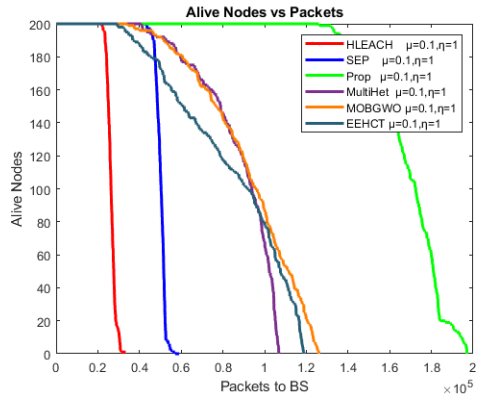

FIGURE 18. Alive Nodes vs Packets to BS in 200 Nodes network.

and $\eta = 1$ of initial energy of advanced nodes while the BS in location (50, 50) and (150, 250). Wherein table 11, the first node died at 983 rounds for HLEACH, 937 round of SEP, 807 round of MultiHet, 892 round of MOBGWO 702 of EEHCT and 1291 rounds of the proposed algorithm for 100 nodes in the network when BS in center, meanwhile the FND is much earlier in scenario 2 where the BS located away from the RoI. The MOBGWO protocol's FND in Scenario 2 is 96.8% lower and the AND is approximately 46.4% lower than the scenario 1. As the same the EEHCT's FND in Scenario 2 is 97.4% and the AND is 20.7% lower than the scenario 1. However, the proposed model's FND in Scenario 2 is 85.7% lower and the AND is approximately 29.4% lower than the scenario 1, it outperforms other models in scenario 2 also.

In scenario 1 200 nodes network, the first node dead if HLEACH is extended to 1003 round, but it is very clear in the table that the other models SEP, MultiHet, MOBGWO, and EEHCT have earlier FND than 100 nodes network. The proposed model demonstrates only a slight increase in the occurrence of the first node failure when transitioning from a 100-node network to a 200-node network. This minor change suggests that the network remains stable and capable of effectively managing larger-scale deployments without significant degradation in performance.

In Scenario 2 of 200 nodes network, the MOBGWO's FND is 96.5% and AND is 51.3% lesser than the scenario 1 200NN. The EEHCT's FND round is 97% and AND round is 16.1% lesser than the scenario 1, in both the models, the higher differnece of FND and AND is due to no proposer routing from source to destination, especially when the destination i.e., BS located far from the sources. Herein the proposed model achieves higher node lifetime prolongation than the other models, which directly reflects on total packet transmission to the BS. In table 17 scenario 2 of 200NN, has HLEACH 28.80196602% SEP 83.89%, MULTI HET has 65.45%, MOBGWO has 37.53% and EEHCT has 37.21% of energy lower than the proposed model at 90 nodes dead.

As the number of first nodes dead is extended, the total number of packets received at the Base Station with respect to rounds is also increased. The packets received at the BS of HLEACH of 100 nodes nework is 74.1%, and 200 nodes network is 76.5% lesser than the proposed model. The other algorithms have higher packet transmission to BS when compared to the same algorithms of 100 nodes to 200 nodes. The proposed model has 27.8% higher than MultiHet, 9.18% higher than MOBGWO and 15.68% higher packets received at the BS in 200 nodes network. The models are further evaluated with average residual energy (ARE) during node failure at the round, as presented in Table 17 for 100 and 200 nodes, respectively. These table offers valuable insights

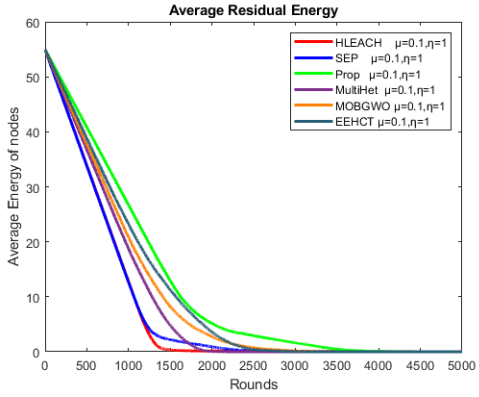

FIGURE 19. Average residual Energy vs Rounds in 100 Node network.

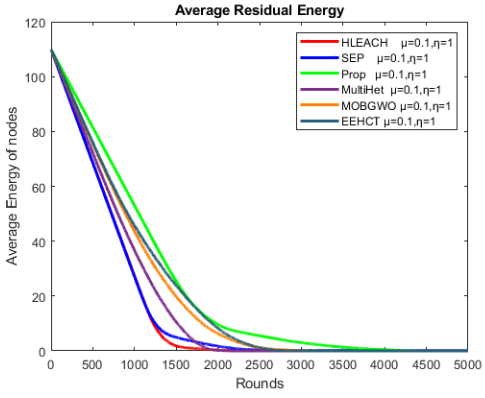

FIGURE 20. Average residual Energy vs Rounds in 200 Node network.

into the duration of node survival within the network and how efficiently the models utilize residual energy to extend the network's lifetime.

2) CASE 2

Case 2 is simulated by varying the energy level of only the advanced nodes as $(1 + \eta)$ where the η is set to 2 i.e., $\mu = 0.1$ and $\eta = 2$. This is to analyze the network performance without increasing the number of advanced nodes, just by only increasing the energy level of advanced nodes.

In the scenario 1 and 2, the first node dead is slightly better for all the protocols but the proposed is performed better than others and also in the number of packet received as in Table 12. The increase in energy of the advanced nodes drastically prolonged the last node dead rounds of all the protocols, which is clearly given in table 12. Table 18 showcases the average residual energy of the 100 node network, where the residual energy of the MultiHet, MOBGWO and EEHCT are higher at the FND because the first node died much earlier than the other models, hence the residual energy is higher. In the further rounds the residual energy of all the models are decreased linearly.

The average residual energy of the proposed network surpasses that of the other protocols. In Table 18, representing a 100-node network, the MultiHet protocol exhibits higher values than other models when 25 nodes fail. However, due

TABLE 11. Case 1:$\mu = 0.1, \eta = 1$: Table of nodes dead and packets received at BS.

CASE=1	Scenario 1: 100 nodes Network when area (100 × 100) and BS in Center (50, 50)										Scenario 2 : 100 nodes Network when area (200 × 200) and BS in Center (150, 250)									
	Round at Node dead					Total number of packet received at BS					Round at Node dead					Total number of packet received at BS				
100	HLEACH	SEP	MULTI HET	MOBGWO	EEHCT	PROP	LEACH	SEP	MULTI HET	MOBGWO	EEHCT	PROP	HLEACH	SEP	MULTI HET	MOBGWO	EEHCT	PROP	LEACH	SEP	MULTI HET	MOBGWO	EEHCT	PROP
FND	983	937	807	892	702	1267	20655	10562	33419	37771	31032	60452	165	160	177	28	18	180	3459	1800	1813	204	193	1799
AND	3674	2572	3614	3775	3286	4243	30791	16232	94781	84405	92071	119245	1852	1578	1486	2021	2604	2993	13266	7783	8654	8870	9255	24324
CASE=1	Scenario 1: 200 Nodes Network										Scenario 2 : 200 Nodes Network									
	Round at Node dead					Total number of packet received at BS					Round at Node dead					Total number of packet received at BS				
200	HLEACH	SEP	MULTI HET	MOBGWO	EEHCT	PROP	HLEACH	SEP	MULTI HET	MOBGWO	EEHCT	PROP	HLEACH	SEP	MULTI HET	MOBGWO	EEHCT	PROP	HLEACH	SEP	MULTI HET	MOBGWO	EEHCT	PROP
FND	1003	938	543	663	456	1295	40657	20649	53234	42228	26812	110324	149	136	183	23	13	176	6078	2916	3792	573	261	2999
AND	3854	2576	2218	3962	3206	4589	60228	32237	98435	119267	110733	131326	2847	2057	1529	1928	2689	2730	27927	16769	15782	11943	11887	69493

TABLE 12. Case 2:$\mu = 0.1, \eta = 2$: Table of nodes dead and packets received at BS.

Scenario 1: 100 nodes Network when area (100 × 100) and BS in Center (50, 50)												
CASE - 2	Round at Node dead						Total number of packet received at BS					
ROUNDS	HLEACH	SEP	MULTI HET	MOBGWO	EEHCT	PROP	LEACH	SEP	MULTI HET	MOBGWO	EEHCT	GNN prop
FND	1013	1250	729	814	536	1279	21267	14256	30505	32824	19016	62012
AND	6430	4438	6096	5498	3710	6893	41242	24650	128855	95260	80108	135689
Scenario 1: 200 Nodes Network												
CASE - 2	Round at Node dead						Total number of packet received at BS					
200	HLEACH	SEP	MULTI HET	MOBGWO	EEHCT	PROP	HLEACH	SEP	MULTI HET	MOBGWO	EEHCT	PROP
FND	1029	1143	437	486	355	1304	42169	23992	26878	33489	20306	122452
AND	4392	3506	3051	3788	3598	6780	63484	35129	104290	139613	121922	162093

Scenario 2 : 100 nodes Network when area (200 × 200) and BS in Center (150, 250)												
CASE - 2	Round at Node dead						Total number of packet received at BS					
HLEACH	SEP	MULTI HET	MOBGWO	EEHCT	PROP	HLEACH	SEP	MULTI HET	MOBGWO	EEHCT	PROP
162	150	192	20	16	217	3400	1654	2386	292	201	1699
4014	4432	2117	2764	2731	**4802**	17764	12330	11111	7864	8275	**30974**
Scenario 2 : 200 Nodes Network												
CASE - 2	Round at Node dead						Total number of packet received at BS					
HLEACH	SEP	MULTI HET	MOBGWO	EEHCT	PROP	HLEACH	SEP	MULTI HET	MOBGWO	EEHCT	PROP
148	189	185	36	17	205	6060	3924	3497	617	314	3397
4116	1476	2085	1499	2385	**4673**	32089	15300	14678	12418	11609	**76862**

TABLE 13. Case 3:$\mu = 0.1, \eta = 5$: Table of nodes dead and packets received at BS.

Scenario 1: 100 nodes Network when area (100 × 100) and BS in Center (50, 50)												
CASE - 3	Round at Node dead						Total number of packet received at BS					
ROUNDS	HLEACH	SEP	MULTI HET	MOBGWO	EEHCT	PROP	LEACH	SEP	MULTI HET	MOBGWO	EEHCT	GNN prop
FND	1026	1428	638	487	475	1287	21536	16080	29585	12671	27542	64785
AND	12011	8917	11127	8877	4525	12962	68435	49804	233313	86754	169778	271145
Scenario 1: 200 Nodes Network												
CASE - 3	Round at Node dead						Total number of packet received at BS					
ROUNDS	HLEACH	SEP	MULTI HET	MOBGWO	EEHCT	PROP	HLEACH	SEP	MULTI HET	MOBGWO	EEHCT	PROP
FND	1043	1192	285	240	239	1324	42725	25273	15282	6284	14751	123453
AND	10623	7241	4083	4531	3940	12945	86039	66377	131436	177677	166656	295542

Scenario 2 : 100 nodes Network when area (200 × 200) and BS in Center (150, 250)												
CASE - 3	Round at Node dead						Total number of packet received at BS					
HLEACH	SEP	MULTI HET	MOBGWO	EEHCT	PROP	LEACH	SEP	MULTI HET	MOBGWO	EEHCT	GNN prop
174	196	159	12	9	328	3682	2184	1248	1638	81	1896
5012	2749	1867	6284	7001	**8648**	22048	9295	8605	12418	11697	**32106**
Scenario 2 : 200 Nodes Network												
CASE - 3	Round at Node dead						Total number of packet received at BS					
HLEACH	SEP	MULTI HET	MOBGWO	EEHCT	PROP	HLEACH	SEP	MULTI HET	MOBGWO	EEHCT	PROP
133	204	174	25	10	318	5463	4308	4558	2646	490	4372
6574	6287	2123	4998	2378	**7196**	43020	30454	24343	31810	15788	**74831**

TABLE 14. Case 4:$\mu = 0.24, \eta = 1$: Table of nodes dead and packets received at BS.

Scenario 1: 100 nodes Network when area (100 × 100) and BS in Center (50, 50)												
CASE - 4	Round at Node dead						Total number of packet received at BS					
ROUNDS	HLEACH	SEP	MULTI HET	MOBGWO	EEHCT	PROP	LEACH	SEP	MULTI HET	MOBGWO	EEHCT	GNN prop
FND	1020	1093	862	1178	950	1317	21420	12027	34385	43378	41132	72584
AND	2930	3256	3857	3918	3328	6519	32028	18283	87105	83943	100782	144369
Scenario 1: 200 Nodes Network												
CASE - 4	Round at Node dead						Total number of packet received at BS					
ROUNDS	HLEACH	SEP	MULTI HET	MOBGWO	EEHCT	PROP	HLEACH	SEP	MULTI HET	MOBGWO	EEHCT	PROP
FND	1043	1094	832	912	670	1355	42789	22946	51716	56196	41244	125412
AND	3739	3557	2438	3755	3467	7540	63863	35524	107425	126891	134120	187677

Scenario 2 : 100 nodes Network when area (200 × 200) and BS in Center (150, 250)												
CASE - 4	Round at Node dead						Total number of packet received at BS					
HLEACH	SEP	MULTI HET	MOBGWO	EEHCT	PROP	LEACH	SEP	MULTI HET	MOBGWO	EEHCT	GNN prop
132	167	149	38	10	223	2784	1832	1968	944	92	2199
3994	3136	1386	1706	1775	**4118**	21448	10392	11894	7740	8528	**34591**
Scenario 2 : 200 Nodes Network												
CASE - 4	Round at Node dead						Total number of packet received at BS					
HLEACH	SEP	MULTI HET	MOBGWO	EEHCT	PROP	HLEACH	SEP	MULTI HET	MOBGWO	EEHCT	PROP
128	165	208	25	9	220	5262	3461	5027	852	117	3998
3547	3154	1456	2250	2529	**3905**	33383	19810	14300	9723	11740	**53998**

TABLE 15. Case 5:$\mu = 0.24, \eta = 2$: Table of nodes dead and packets received at BS.

Scenario 1: 100 nodes Network when area (100 × 100) and BS in Center (50, 50)												
CASE - 5	Round at Node dead						Total number of packet received at BS					
ROUNDS	HLEACH	SEP	MULTI HET	MOBGWO	EEHCT	PROP	LEACH	SEP	MULTI HET	MOBGWO	EEHCT	PROP
FND	1013	1250	729	969	801	1336	21267	14256	30505	42227	28894	65887
AND	6430	4438	6096	3950	5174	8625	41242	24650	128855	114058	102742	182045
Scenario 1: 200 Nodes Network												
CASE - 5	Round at Node dead						Total number of packet received at BS					
ROUNDS	HLEACH	SEP	MULTI HET	MOBGWO	EEHCT	PROP	HLEACH	SEP	MULTI HET	MOBGWO	EEHCT	PROP
FND	1018	1238	1029	1176	874	1362	41728	25662	66553	76868	60917	126939
AND	9446	4051	4713	4046	4154	9771	75490	45832	142484	165946	176503	262045

Scenario 2 : 100 nodes Network when area (200 × 200) and BS in Center (150, 250)												
CASE - 5	Round at Node dead						Total number of packet received at BS					
HLEACH	SEP	MULTI HET	MOBGWO	EEHCT	PROP	LEACH	SEP	MULTI HET	MOBGWO	EEHCT	PROP
153	182	165	41	12	325	3229	2065	1982	1817	108	2470
4982	5729	2379	3328	4902	**5323**	25140	16886	12618	11017	13993	**32987**
Scenario 2 : 200 Nodes Network												
CASE - 5	Round at Node dead						Total number of packet received at BS					
HLEACH	SEP	MULTI HET	MOBGWO	EEHCT	PROP	HLEACH	SEP	MULTI HET	MOBGWO	EEHCT	PROP
179	171	258	52	10	319	7343	3731	5084	2588	170	3982
4862	4863	1689	2552	3018	**4983**	42786	24487	18720	14332	13222	**77741**

TABLE 16. Case 6:$\mu = 0.24, \eta = 5$: Table of nodes dead and packets received at BS.

Scenario 1: 100 nodes Network when area (100 × 100) and BS in Center (50, 50)													Scenario 2 : 100 nodes Network when area (200 × 200) and BS in Center (150, 250)											
CASE - 6	Round at Node dead						Total number of packet received at BS						CASE - 6	Round at Node dead							Total number of packet received at BS					
ROUNDS	HLEACH	SEP	MULTI HET	MOBGWO	EEHCT	PROP	HLEACH	SEP	MULTI HET	MOBGWO	EEHCT	PROP	HLEACH	SEP	MULTI HET	MOBGWO	EEHCT	PROP	LEACH	SEP	MULTI HET	MOBGWO	EEHCT	PROP
FND	1026	1428	638	341	442	1351	21536	16080	29585	3768	33150	78554	175	258	191	24	20	320	3681	2864	1382	480	140	2097
AND	13011	8917	10127	12443	10294	14761	68435	49804	233313	209716	222465	290429	9041	8144	3569	9225	2863	**8918**	40025	27878	13411	7382	11548	**44391**
Scenario 1: 200 Nodes Network													Scenario 2 : 200 Nodes Network											
CASE - 6	Round at Node dead						Total number of packet received at BS						CASE - 6	Round at Node dead							Total number of packet received at BS					
ROUNDS	HLEACH	SEP	MULTI HET	MOBGWO	EEHCT	PROP	HLEACH	SEP	MULTI HET	MOBGWO	EEHCT	PROP	HLEACH	SEP	MULTI HET	MOBGWO	EEHCT	PROP	HLEACH	SEP	MULTI HET	MOBGWO	EEHCT	PROP
FND	1036	1406	259	270	144	1372	42482	28776	12372	11607	4073	138675	160	271	281	61	13	319	6554	5820	3705	1452	169	3995
AND	14126	8677	13993	13957	13320	14683	115304	95535	252844	327634	292485	421233	8193	8058	8120	7754	7924	**8316**	56943	41474	21865	25712	32536	**92199**

TABLE 17. Case 1:$\mu = 0.1, \eta = 1$: ARE of network during number of node dead at round.

Scenario 1: 100 nodes Network when area (100 × 100) and BS in Center (50, 50)													Scenario 2 : 100 nodes Network when area (200 × 200) and BS in Center (150, 250)											
Case - 1	Node dead round						Average residual Energy during node dead						Case - 1	Node dead round						Average residual Energy during node dead					
Node dead	HLEACH	SEP	MULTI HET	MOBGWO	EEHCT	PROP	HLEACH	SEP	MULTI HET	MOBGWO	EEHCT	PROP	HLEACH	SEP	MULTI HET	MOBGWO	EEHCT	PROP	HLEACH	SEP	MULTI HET	MOBGWO	EEHCT	PROP
1	983	937	807	892	702	1267	13.63631	15.60018	32.21298	25.75719	33.7434	17.58682	165	160	177	28	18	180	34.10295	35.15409	35.81093	45.10352	45.56134	36.34492
25	1159	1224	1269	1375	1356	1508	7.65066	3.782073	16.15378	14.5374	15.84588	10.01795	309	335	364	82	67	346	19.50445	19.04184	18.83512	26.45374	26.11696	23.6287
50	1242	1332	1535	1743	1865	1767	5.13763	1.725953	6.916566	8.262438	6.232733	7.805755	479	560	588	160	167	700	10.29173	8.208522	8.158885	12.9038	13.77873	8.822722
70	1295	1389	1777	1976	2280	1982	3.895482	0.630856	3.587809	2.59133	1.865131	5.690756	640	757	738	308	308	976	5.361052	3.419449	3.827056	5.411939	7.466642	6.377908
90	1508	1485	1947	2513	2691	2494	2.116906	0.183509	0.605143	0.545495	0.223367	2.655293	1065	1044	958	802	919	1632	1.573193	0.355775	0.763373	1.380299	1.387241	2.209601
Scenario 1: 200 Nodes Network													Scenario 2: 200 Nodes Network											
Case - 1	Node dead round						Average residual Energy during node dead						Case - 1	Node dead round						Average residual Energy during node dead					
Node dead	HLEACH	SEP	MULTI HET	MOBGWO	EEHCT	PROP	HLEACH	SEP	MULTI HET	MOBGWO	EEHCT	PROP	HLEACH	SEP	MULTI HET	MOBGWO	EEHCT	PROP	HLEACH	SEP	MULTI HET	MOBGWO	EEHCT	PROP
1	1033	938	543	663	456	1259	24.4871	32.4292	68.9398	64.1745	78.6955	37.8286	149	136	183	23	13	176	74.6078	75.7895	74.8074	88.4759	90.8201	75.018
50	1171	1213	1187	1216	1069	1644	14.1858	10.8562	26.3137	30.53	42.1146	18.4166	330	317	426	75	45	353	43.9765	41.6538	35.7196	58.7612	58.8327	49.4769
100	1267	1300	1525	1594	1624	1856	9.36192	6.25127	10.4125	14.4142	18.8924	12.0619	609	588	583	156	143	767	18.8066	18.9341	19.1861	36.3872	32.6254	20.0986
150	1348	1426	1814	2007	2191	2099	6.9595	2.4915	2.14052	5.02414	4.87862	8.00166	898	933	873	499	555	1003	6.68897	4.99467	5.39229	9.72605	10.7511	8.48994
190	2218	1593	2016	2842	2965	3522	0.83615	1.00466	0.1967	0.60359	0.04675	0.94902	1224	1288	1132	1192	1303	1523	2.35298	0.85025	0.70284	0.21196	1.94327	2.44719

TABLE 18. Case 2:$\mu = 0.1, \eta = 2$: ARE of network during number of node dead at round.

Scenario 1: 100 nodes Network when area (100 × 100) and BS in Center (50, 50)													Scenario 2 : 100 nodes Network when area (200 × 200) and BS in Center (150, 250)											
Case - 2	Node dead round						Average residual Energy during node dead						Case - 2	Node dead round					Average residual Energy during node dead					
node dead	HLEACH	SEP	MULTI HET	MOBGWO	EEHCT	PROP	HLEACH	SEP	MULTI HET	MOBGWO	EEHCT	PROP	HLEACH	SEP	MULTI HET	MOBGWO	EEHCT	PROP	HLEACH	SEP	MULTI HET	MOBGWO	EEHCT	PROP
1	1013	1250	729	814	536	1304	18.51571	15.93652	45.31788	32.92549	42.45696	21.7749	162	150	192	20	16	217	39.12182	41.61204	39.7245	49.71574	52.77003	37.4089
25	1145	1313	1207	1279	1343	1629	11.75068	6.242753	**23.8485**	19.62018	19.38408	18.1383	294	315	461	83	54	557	26.44546	25.04463	**17.1148**	30.72186	32.14678	29.3206
50	1228	1378	1629	1721	1983	1811	9.789783	4.347238	13.53766	11.23203	6.95857	15.7991	489	611	607	261	94	819	16.47007	10.6855	10.02935	15.10001	21.81678	9.6167
70	1339	1432	1897	2359	2367	2117	8.638207	2.913366	8.000752	4.584493	2.558553	11.2629	801	874	816	428	338	1062	7.775642	4.203039	4.185593	9.343209	9.356423	6.70975
90	1548	1582	2275	3394	2834	2502	**6.95664**	1.890131	1.307287	1.169766	0.466145	7.94287	1079	1165	1044	912	871	1827	2.627606	1.179033	1.18121	1.684627	2.379751	2.97018
Scenario 1: 200 Nodes Network													Scenario 2: 200 Nodes Network											
Case - 2	Node dead round						Average residual Energy during node dead						Case - 2	Node dead round					Average residual Energy during node dead					
node dead	HLEACH	SEP	MULTI HET	MOBGWO	EEHCT	PROP	HLEACH	SEP	MULTI HET	MOBGWO	EEHCT	PROP	HLEACH	SEP	MULTI HET	MOBGWO	EEHCT	PROP	HLEACH	SEP	MULTI HET	MOBGWO	EEHCT	PROP
1	1029	1143	437	486	355	1279	34.8907	25.4304	86.1759	86.6857	95.5601	47.3493	148	189	185	36	17	205	81.3653	76.1651	79.5487	94.7391	96.9889	76.1295
50	1172	1289	1246	1356	1231	1631	24.4157	14.852	30.9144	34.8327	**42.6698**	30.0768	269	416	430	155	50	552	57.208	37.5639	36.3773	47.1757	**63.8109**	45.9715
100	1263	1413	1695	1818	1801	1844	19.8443	8.99916	8.97177	15.1184	19.5104	23.2348	549	593	592	259	147	741	29.6332	21.5526	20.6253	5.56726	32.5985	30.6331
150	1401	1515	1921	2271	2448	2080	15.9566	6.27285	2.69941	5.2109	4.10263	18.7055	866	972	875	510	457	1034	15.7563	3.93958	6.81844	1.45305	10.7615	20.7195
190	3436	2273	2192	2986	2962	5475	1.50812	1.26514	0.66828	0.38227	0.24909	1.48054	1370	1169	1296	1043	1259	1536	5.17816	0.75601	0.49461	0.5384	1.47856	4.30268

TABLE 19. Case 3:$\mu = 0.1, \eta = 5$: ARE of network during number of node dead at round.

Scenario 1: 100 nodes Network when area (100 × 100) and BS in Center (50, 50)													Scenario 2 : 100 nodes Network when area (200 × 200) and BS in Center (150, 250)											
Case - 3	Node dead round						Average residual Energy during node dead						Case - 3	Node dead round					Average residual Energy during node dead					
node dead	HLEACH	SEP	MULTI HET	MOBGWO	EEHCT	PROP	HLEACH	SEP	MULTI HET	MOBGWO	EEHCT	PROP	HLEACH	SEP	MULTI HET	MOBGWO	EEHCT	PROP	HLEACH	SEP	MULTI HET	MOBGWO	EEHCT	PROP
1	1026	1428	638	487	475	1287	33.0121	24.3312	48.0673	55.733	62.4253	39.6705	174	196	159	12	9	328	55.7071	48.1733	60.1485	68.142	70.9914	50.6854
25	1149	1440	1944	1781	2562	1631	26.8621	15.6812	**23.4315**	14.4396	11.4236	35.1355	395	410	515	106	250	548	37.8448	25.3006	**24.1484**	51.4041	50.5611	26.8533
50	1230	1515	2133	2114	2894	1767	25.242	12.9074	13.7936	7.44659	5.62084	28.9316	628	654	841	384	337	942	25.4613	12.3552	10.9518	29.5434	35.8078	22.6086
70	1302	1617	2257	2394	3218	3106	23.9238	10.8278	6.19946	4.29002	2.26116	25.0544	776	849	1106	682	907	1283	19.9954	6.45873	3.15501	15.8534	14.5567	17.3966
90	1503	2225	2381	3329	3635	4595	**21.642**	9.40842	1.34786	0.62382	0.30601	24.4682	1199	1127	1327	1716	2187	3813	3.70288	2.4354	0.40768	4.5257	4.75582	7.20073
Scenario 1: 200 Nodes Network													Scenario 2 : 200 Nodes Network											
Case - 3	Node dead round						Average residual Energy during node dead						Case - 3	Node dead round					Average residual Energy during node dead					
node dead	HLEACH	SEP	MULTI HET	MOBGWO	EEHCT	PROP	HLEACH	SEP	MULTI HET	MOBGWO	EEHCT	PROP	HLEACH	SEP	MULTI HET	MOBGWO	EEHCT	PROP	HLEACH	SEP	MULTI HET	MOBGWO	EEHCT	PROP
1	1043	1192	285	240	239	1244	63.4733	51.3361	127.495	130.224	133.918	77.9453	133	204	174	25	10	318	121.154	104.168	113.957	134.165	142.504	123.391
50	1161	1352	1866	1972	1931	1593	54.7505	39.546	13.0571	30.7901	**31.388**	60.0941	368	446	414	179	119	454	83.2191	60.324	73.903	83.6102	**99.6727**	93.6441
100	1244	1470	2056	2409	2344	3786	50.5338	33.3373	4.92685	13.2131	14.7556	53.6331	653	705	833	413	340	861	48.0533	36.1313	28.1508	40.8926	60.0711	60.6517
150	1360	1679	2203	2808	2820	4148	47.2247	26.9919	1.57397	4.30757	4.03926	47.7226	970	1188	1190	731	1164	1173	32.2887	13.6458	10.5355	17.9344	10.6298	37.7243
190	7165	5163	2321	3446	3434	10757	3.02846	2.83219	0.65203	0.34348	0.2626	2.71782	2331	1817	1394	1416	1879	3282	9.74951	6.16879	5.81307	3.59128	0.69681	9.46186

TABLE 20. Case 4:$\mu = 0.24, \eta = 1$: ARE of network during number of node dead at round.

Scenario 1: 100 nodes Network when area (100 × 100) and BS in Center (50, 50)												
Case - 4	Node dead round						Average residual Energy during node dead					
node dead	HLEACH	SEP	MULTI HET	MOBGWO	EEHCT	PROP	HLEACH	SEP	MULTI HET	MOBGWO	EEHCT	PROP
1	1020	1093	862	1178	950	1397	16.9919	13.6569	34.9081	21.9486	33.2517	23.31555
25	1184	1335	1501	1574	1576	1694	10.9924	7.15893	**19.632**	10.2267	16.4931	15.93403
50	1303	1413	1728	1785	2103	1952	8.16423	4.2608	8.53064	6.29016	6.58569	11.9618
70	1392	1448	1874	2080	2503	2249	6.5134	3.36783	3.8172	3.13927	2.26995	8.937037
90	2396	1774	2068	2799	2923	3689	**0.39886**	0.80554	0.77301	0.50046	0.32509	1.930541

Scenario 2 : 100 nodes Network when area (200 × 200) and BS in Center (150, 250)												
Case - 4	Node dead round						Average residual Energy during node dead					
HLEACH	SEP	MULTI HET	MOBGWO	EEHCT	PROP	HLEACH	SEP	MULTI HET	MOBGWO	EEHCT	PROP
132	167	149	38	10	223	43.5982	39.9637	44.8294	46.9496	49.2807	44.02804
322	374	525	150	39	354	26.245	21.8474	**17.1137**	24.6045	33.3727	24.79887
619	622	769	316	154	755	12.7213	9.95034	6.88752	11.5546	16.9333	14.19227
892	864	928	478	424	1353	5.64027	3.56829	2.79719	4.85294	8.07479	10.36275
1210	1164	1224	809	1107	2743	2.17516	0.75696	0.11485	0.7534	0.77658	2.332028

Scenario 1: 200 Nodes Network												
Case - 4	Node dead round						Average residual Energy during node dead					
node dead	HLEACH	SEP	MULTI HET	MOBGWO	EEHCT	PROP	HLEACH	SEP	MULTI HET	MOBGWO	EEHCT	PROP
1	1043	1094	832	912	670	1345	37.6252	33.491	60.1154	60	79.3865	47.9859
50	1188	1350	1393	1479	1377	1646	26.8593	15.0938	22.0229	25.5023	**39.1842**	33.2292
100	1311	1394	1694	1798	1958	1921	20.977	13.1424	7.69573	11.8643	16.2784	24.318
150	1523	1616	1917	2113	2493	2293	15.2736	7.29085	1.59338	4.44233	4.07416	17.6703
190	2530	2239	2078	2763	2990	4258	0.38493	0.81175	0.2413	0.85762	0.20316	1.34008

Scenario 2: 200 Nodes Network												
Case - 4	Node dead round						Average residual Energy during node dead					
HLEACH	SEP	MULTI HET	MOBGWO	EEHCT	PROP	HLEACH	SEP	MULTI HET	MOBGWO	EEHCT	PROP
128	165	208	25	9	220	91.4298	83.8928	81.8711	96.2769	105.568	88.4513
412	441	465	85	62	448	43.4413	40.9693	39.2749	58.619	**60.4999**	39.7694
639	683	712	216	163	717	23.6338	22.3152	16.5833	29.2588	33.4983	34.8014
944	1047	946	481	463	1318	8.80824	7.85328	5.46967	8.97743	14.5	15.4741
1360	1602	1204	1206	1578	2087	1.83123	1.01766	0.34036	0.61811	0.70495	1.80896

TABLE 21. Case 5:$\mu = 0.24, \eta = 2$: ARE of network during number of node dead at round.

Scenario 1: 100 nodes Network when area (100 × 100) and BS in Center (50, 50)												
Case - 5	Node dead round						Average residual Energy during node dead					
node dead	HLEACH	SEP	MULTI HET	MOBGWO	EEHCT	PROP	HLEACH	SEP	MULTI HET	MOBGWO	EEHCT	PROP
1	1013	1250	729	969	801	1242	27.17321	17.01351	52.13171	43.4547	47.84731	38.22651
25	1186	1408	1742	1853	1175	1629	20.75756	12.16741	**24.33743**	19.11007	36.18425	28.43392
50	1296	1558	1980	2517	2462	1925	18.30896	8.919479	13.67085	7.01127	7.081475	23.69436
70	1391	1630	2189	2941	2773	2284	15.93985	7.884431	9.291542	2.303493	3.40062	20.07461
90	3562	2799	2807	3309	3352	5559	**0.867854**	1.539181	0.53135	0.560579	1.101552	2.871347

Scenario 2 : 100 nodes Network when area (200 × 200) and BS in Center (150, 250)												
Case - 5	Node dead round						Average residual Energy during node dead					
HLEACH	SEP	MULTI HET	MOBGWO	EEHCT	PROP	HLEACH	SEP	MULTI HET	MOBGWO	EEHCT	PROP
153	182	165	41	12	325	53.32897	49.12338	52.4063	59.90104	59.88941	50.87954
441	491	545	223	48	554	29.26861	24.35624	**19.38795**	31.75041	43.25037	40.2595
679	811	766	475	161	855	17.67868	11.82774	9.693846	14.29061	26.24868	21.36933
886	998	955	663	424	1303	12.17675	7.261307	5.10384	6.786147	13.7159	13.03044
1505	1307	1263	995	1504	2801	3.883576	3.789174	1.780255	1.633276	2.710467	3.900969

Scenario 1: 200 Nodes Network												
Case - 5	Node dead round						Average residual Energy during node dead					
node dead	HLEACH	SEP	MULTI HET	MOBGWO	EEHCT	PROP	HLEACH	SEP	MULTI HET	MOBGWO	EEHCT	PROP
1	1018	1238	1029	1176	874	1322	63.6977	45.6098	69.5453	67.3463	91.1765	72.3554
50	1187	1411	1775	1856	1882	1667	51.2853	32.9161	18.0228	27.1605	**34.1436**	55.2952
100	1274	1559	1966	2147	2356	3898	46.9911	25.2465	8.95515	16.0943	15.6159	48.1194
150	1509	2039	2096	2611	2830	3226	40.406	14.601	5.29819	5.4178	4.18324	41.8473
190	3848	3113	2712	3344	3489	6140	8.12916	0.95889	1.3622	0.45945	0.23506	2.65344

Scenario 2: 200 Nodes Network												
Case - 5	Node dead round						Average residual Energy during node dead					
HLEACH	SEP	MULTI HET	MOBGWO	EEHCT	PROP	HLEACH	SEP	MULTI HET	MOBGWO	EEHCT	PROP
179	171	258	52	10	319	102.613	100.924	91.4832	92.6747	120.238	101.166
459	478	581	115	53	560	62.3616	50.0853	41.4907	66.707	**71.6342**	69.0034
778	829	834	226	111	842	35.5953	19.9219	17.8407	44.6457	47.5888	51.3718
1058	1094	1113	735	507	1283	22.5658	8.38118	4.66523	11.7022	13.2335	19.6802
2665	1446	1316	1352	1606	2605	1.98492	3.06544	0.43407	0.90971	1.40641	3.12292

TABLE 22. Case 6:$\mu = 0.24, \eta = 5$: ARE of network during number of node dead at round.

Scenario 1: 100 nodes Network when area (100 × 100) and BS in Center (50, 50)												Scenario 2 : 100 nodes Network when area (200 × 200) and BS in Center (150, 250)											
Case - 6	Node dead round					Average residual Energy during node dead						Case - 6	Node dead round					Average residual Energy during node dead					
node dead	HLEACH	SEP	MULTI HET	MOBGWO	EEHCT	PROP	HLEACH	SEP	MULTI HET	MOBGWO	EEHCT	PROP	HLEACH	SEP	MULTI HET	MOBGWO	EEHCT	PROP	HLEACH	SEP	MULTI HET	MOBGWO	EEHCT	PROP
1	1026	1428	638	341	442	1311	56.69815	39.83128	85.70085	95.17818	100.3163	71.98214	175	258	191	24	20	320	81.05801	65.90775	80.37692	90.04875	94.4745	84.62389
25	1290	1639	1210	1988	2906	1651	51.38582	33.49362	**41.88429**	51.73549	34.11537	63.45732	379	494	661	105	165	550	65.42707	44.01181	**44.9988**	74.62	67.5822	70.48492
50	1344	1741	1344	2627	3553	2877	47.50674	30.11739	22.08778	39.63423	21.30616	59.81237	636	758	1024	635	353	877	54.18346	31.18287	29.11768	42.175	42.42209	40.00746
70	1424	1877	1424	3398	4104	4153	46.88649	**28.39531**	9.607634	32.91948	14.99357	56.94924	952	1147	1365	1135	1253	2326	45.44195	19.39058	15.38656	28.09894	13.61543	27.59377
90	7127	7173	7727	9081	4733	10959	**2.327159**	2.247001	1.701415	11.63871	13.55019	5.561026	4865	1715	1867	2587	2362	5876	6.40472	12.76865	8.741099	7.992909	0.575564	2.724122
Scenario 1: 200 Nodes Network												Scenario 2: 200 Nodes Network											
Case - 6	Node dead round					Average residual Energy during node dead						Case - 6	Node dead round					Average residual Energy during node dead					
node dead	HLEACH	SEP	MULTI HET	MOBGWO	EEHCT	PROP	HLEACH	SEP	MULTI HET	MOBGWO	EEHCT	PROP	HLEACH	SEP	MULTI HET	MOBGWO	EEHCT	PROP	HLEACH	SEP	MULTI HET	MOBGWO	EEHCT	PROP
1	1036	1406	259	270	144	1312	134.228	103.317	198.599	199.172	208.997	144.969	160	271	281	61	13	319	163.201	128.381	152.725	177.306	173.738	160.888
50	1157	1577	1971	2129	3051	1675	125.171	90.5738	80.012	94.8564	**38.9595**	127.221	356	502	724	195	85	560	129.306	84.6095	91.7114	130.97	**124.869**	117.742
100	1276	1696	2237	2776	3630	2921	118.933	84.5232	67.4962	70.7615	17.0725	119.427	756	985	1067	381	164	913	89.203	38.613	58.0969	85.3495	75.4944	81.1848
150	1508	2152	2392	3713	4204	4262	112.042	73.5762	63.1691	54.2658	8.1915	112.996	1119	1305	1428	687	653	2552	64.988	23.3363	35.2379	35.8738	47.1557	39.8969
190	7707	6827	11454	13143	4916	12430	1.89999	0.890038	2.97595	5.96416	6.29334	5.14347	3670	2417	2291	1574	2618	3446	8.03715	10.6635	13.3375	10.6207	5.53638	10.3741

to inadequate energy management, the network's longevity is compromised compared to the proposed algorithm. Similarly, in a 200-node network, the EEHCT protocol demonstrates higher residual energy than other models when 50 nodes fail. Nonetheless, the network's lifetime is shortened due to multiple packet transmissions, resulting in premature failure. The proposed model has sustained for longer duration than the other models.

In scenario 2 of 100NN and 200NN, the average residual energy when the 90 nodes dead of HLEACH is 11.5% lower than the proposed model of 100NN and 20.34% higher than the proposed model in 200NN, due to improper energy management all nodes are died earlier at 4116 round. The SEP is 60.30% lesser in 100NN and 82.42% lesser, MULTI HET is 60.23% in 100NN and 88.50% in 200NN, MOBGWO is 43.2% and 87.48% than the proposed model's ARE.

3) CASE 3

Case 3, with $\mu = 0.1$ and $\eta = 5$, is simulated by adjusting the energy level of only the advanced nodes to $(1+\eta)$, where η is set to 5. This analysis aims to evaluate network performance without increasing the quantity of advanced nodes, solely by raising the energy level of advanced nodes to five times that of normal nodes.

Here, only the energy of the advanced nodes has been increased, resulting in the earlier depletion of normal nodes similar to Case 2. The proposed system significantly prolongs the average residual energy of the network compared to other protocols in scenario 1 and 2, as demonstrated in Table 13 and 19. In scenario 1 of a 100-node network, the proposed system's average residual energy when 90 nodes are dead is 11.5% higher than HLEACH, 61.5% higher than SEP, 94.4% higher than MultiHet, 97.9% higher than MOBGWO, and 98.7% higher than EEHCT. In scenario 2 of a 200-node network, although HLEACH and SEP have 11.4% and 4.2% higher average residual energy respectively compared to the proposed model, 190 nodes are dead by the 7165th round for HLEACH and 5163rd round for SEP, clearly indicating the superiority of the proposed model in prolonging network lifetime. Moreover, MultiHet is 76% lower, MOBGWO is 87.3% lower, and EEHCT is 90.3% lower than the proposed model. Therefore, the proposed system efficiently manages the average residual energy in 100 and 200 nodes network. In the scenario 2 of 100NN when compared with the proposed model, the HLEACH has 48.57% lower ARE at 90 nodes dead and AND at round 5012. The SEP has 66.17% lower ARE at 90 nodes dead and AND at round 2749, the MULTIHET has 94.33% lower ARE at 90 nodes dead and AND at round 1867. The MOBGWO has 37.14% lower ARE at 90 nodes dead and AND at round 6284, and the EEHCT has 33.95% lower ARE at 90 nodes dead and AND at round 7001.

4) CASE 4

Case 4 is to analyse the performance of the network by increasing the fraction of advanced nodes. In this scenario,

all networks consist of 100 nodes, with 20 nodes designated as advanced nodes, achieved by setting $\mu = 0.2$. The energy allocated to advanced nodes is adjusted to $(1 + \eta)$, where η is equal to 1, i.e., $\mu = 0.2$ and $\eta = 1$. This configuration is maintained for both the scenarios of 1 and 2 in 100-node and 200-node networks.

The performance of all protocols surpasses that of Case 3, yet the proposed modes exhibit notably higher efficiency than the others in table 14. When comparing Case 3 and Case 4, HLEACH and SEP experience earlier First Node Death (FND) than in Case 3, while other models have a higher number of rounds before FND. Hence, solely increasing the energy level of advanced nodes may extend network lifetime, but augmenting the number of advanced nodes with lower energy levels also enhances network stability.

From the average residual energy table 20 of scenario 1 of 100NN, the proposed model has 57.13% than the HLEACH, 13.43% than the SEP, 16.93% than the MultiHet, 46.2% than the MOBGWO and 65.06% than the EEHCT higher residual energy when the 90^{th} node dead in 100 nodes network. In 200 nodes network, the HLEACH, SEP and the MOBGWO are higher than the proposed model but the 190 nodes are dead half a way to proposed model. The proposed model outperforms the other models, as depicted in Tables 17 and 18. This case demonstrates that increasing the number of advanced nodes is marginally more advantageous than increasing the energy of advanced nodes alone. Therefore, instead of solely elevating the energy level of advanced nodes, augmenting their number with lower energy levels also contributes to increased network stability. On the other side the scenario 2 of 100NN, the ARE of MULTI HET is 64.06% lower, MOBGWO is 56.45% lower, EEHCT is 46.6% lower, and proposed model is 36.83% lower when compares to scenario 1 FND round. However in scenario 2 of 100NN, the proposed model has higher packet reception at the BS by 37.99% than HLEACH 69.95% than SEP, 65.61% than MultiHet, 77.62% than MOBGWO and 75.34% than EEHCT.

5) CASE 5

Case 5 is done on $\mu = 0.2$ and $\eta = 2$. When we increase the number of advanced nodes as well as the energy in Case 2, the network performance is increased, though the first node of the proposed algorithm is earlier than the other, the last node dead is much greater than the other protocol. Tables 15 and 21 prove that the proposed algorithm is prolonging the network lifetime than the other networks.

In table 15 of the 100 node network and the 200 node network, the proposed model FND is at 1336 and 1362 rounds which are not achieved by the other protocols in the present as well as the previous cases. The packets received at the BS in scenario 1 from FND to AND of the protocols are HLEACH 77.3%, SEP 86.4%, MultiHet 29.2%, MOBGWO 37.3%, EEHCT 43.5% and Proposed model 63.8% in 100 nodes network, and in 200 nodes network, the packets received at the BS from FND to AND of the protocols are, HLEACH 71.1%, SEP 82.5%, MultiHet 45.6%, MOBGWO 36.6%, EEHCT 32.64%, and Proposed model 51.5%.

In scenario 2 of 100NN, the total packet received by the HLEACH is 23.7%, SEP is 48.8%, MultiHet is 61.7%, MOBGWO is 66.6% and EEHCT is 57.5% lesser than the proposed model and in 200NN, the total packet received by the HLEACH is 44.9%, SEP is 68.5%, MultiHet is 75.9%, MOBGWO is 81.5% and EEHCT is 82.9% lesser than the proposed model.

In the average residual energy table 21 of scenario 1 for a 100-node network, the proposed model showcases a scenario where 90 nodes expire by the 5559th round. Comparatively, the residual energy of the proposed model surpasses that of HLEACH by 0.4%, MultiHet by 39.02%, and MOBGWO by 35.6%. While SEP and EEHCT demonstrate higher residual energy, but the proposed model extends the lifespan of these nodes significantly. For instance, in the case of SEP, the 90 nodes reach the end of their lifespan by the 2799th round, whereas for EEHCT, it's by the 3352nd round. This observation underscores how the proposed model effectively prolongs the lifespan of nodes compared to other models.

In scenario 1 of the 200 node network, the residual energy of the proposed model os much higher than the other model when 50, 100, and 150 nodes dead, whereas the AND at 6771 round in the proposed model, which is much higher than the other models.

In Scenario 2, involving both 100-node and 200-node networks, table 21 shows the ARE for various models, along with the corresponding AND rounds. While all models demonstrated reduced performance compared to Scenario 1, the proposed model still outperformed the others within this challenging scenario. Specifically, the proposed model able to extend network lifetime up to 5323 rounds for the 100-node network and 4983 rounds for the 200-node network, indicating its robustness in maintaining network stability even under conditions of overall reduced efficiency.

6) CASE 6

This case is simulated by elevating the energy parameter, denoted as $\eta = 5$, for the advanced nodes, while maintaining $\mu = 0.2$, to assess the performance of all protocols under this configuration, where both parameters are set as $\mu = 0.2$ and $\eta = 5$ for 100 node network and 200 node network.

In scenario 1 stated in table 16 and 22 of Case 6, the SEP protocol demonstrates a FND occurring at 1428 rounds in the 100-node network and 1406 rounds in the 200-node network, accompanied by an average residual energy of $39.8J$ and $103.3J$ respectively, both significantly lower than the other models. On the other hand, the MultiHet protocol exhibits average residual energies of $85.7J$ in the 100-node network and $198.5J$ in the 200-node network, while experiencing FND at 638 rounds and 259 rounds respectively. Similarly, MOBGWO displays average residual energies of $95.1J$ in the 100-node network and $199.1J$ in the 200-node network, with corresponding FNDs at 341 rounds and 270 rounds. Lastly, EEHCT shows average residual energies of $100.3J$

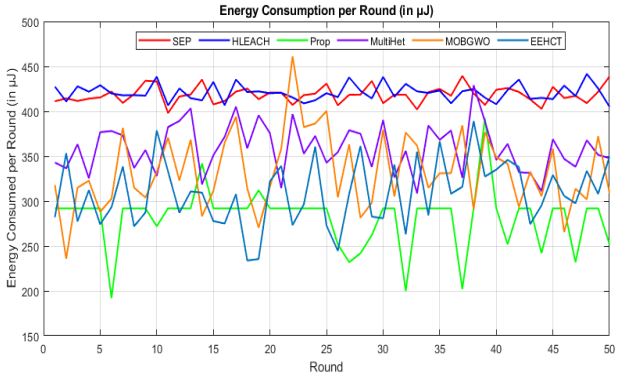

(a) Average Energy Consumption in Scenario 1

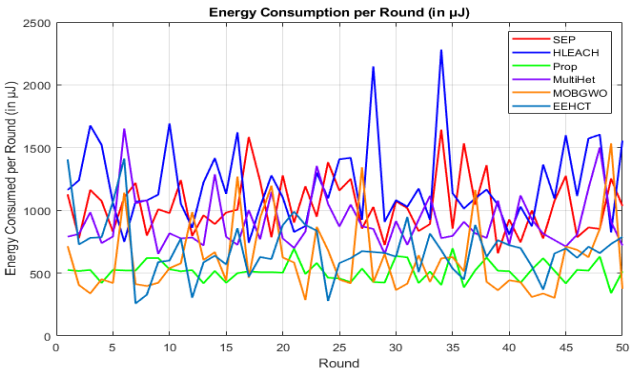

(b) Average Energy Consumption in Scenario 2

FIGURE 21. Average energy consumption per round.

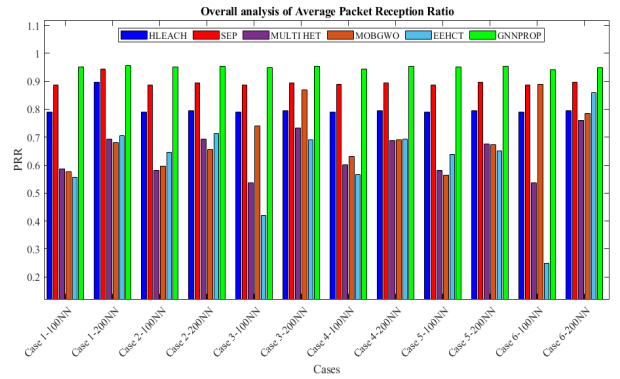

(a) Average PRR in Scenario 1

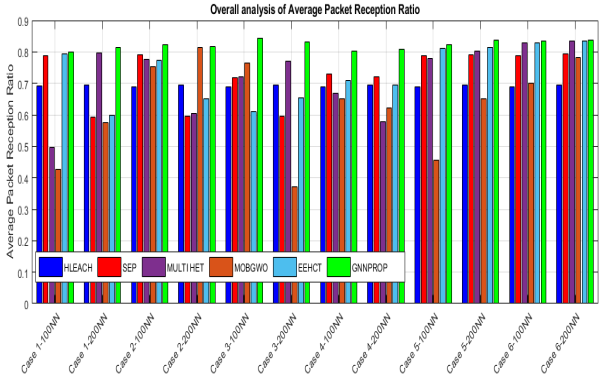

(b) Average PRR in Scenario 2

FIGURE 22. Packet reception ratio at BS.

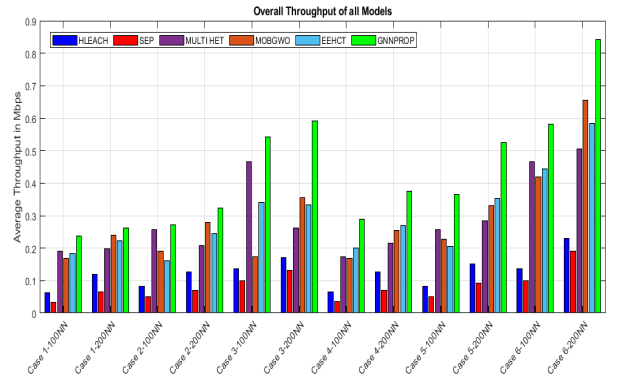

(a) Average of Throughput in Scenario 1

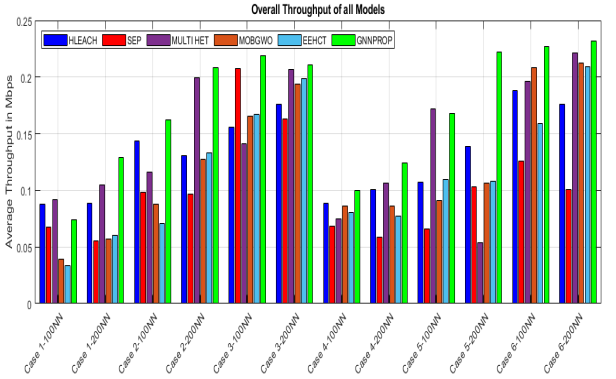

(b) Average of Throughput in Scenario 2

FIGURE 23. Average of throughput in Mbps.

in the 100-node network and 208.9*J* in the 200-node network, along with FNDs at 442 rounds and 144 rounds respectively. HLeach demonstrates moderately competitive performance, although it does not reach the level achieved by the proposed model. In scenario 2 of 100NN and 200NN compared with scenario 1, the packets received at BS in scenario 2 is totally reduced due to the distance from the nodes to BS, however the proposed model has 9.83 higher

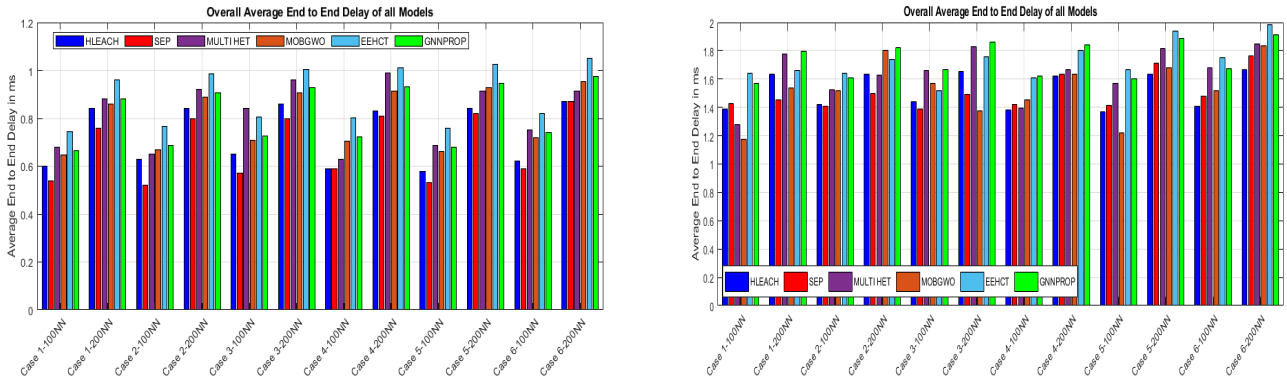

(a) End to End Delay in Scenario 1

(b) End to End Delay in Scenario 2

FIGURE 24. Average End to End Delay in milliseconds.

than HLEACH, 37.1% higher than SEP, 69.7% higher than MultiHet, 83.3% than the MOBGWO and 73.9% than the EEHCT in 100NN of scenario 2. The proposed model has 38.2 higher than HLEACH, 55% higher than SEP, 76.2% higher than MultiHet, 72.1% than the MOBGWO and 64.7% than the EEHCT in 200NN of scenario 2 table 16.

In the comparison of the rounds at which all nodes dead in scenario 1, HLEACH leads with 9896 rounds, followed closely by SEP with 8677 rounds. MultiHet lags significantly behind with nodes dying at 13993 rounds, while PBOFFA, and IDSHR, exhibit similar performance, with nodes ceasing to function at approximately 12957, and 13320 rounds respectively. This data suggests that HLEACH and SEP maintain a longer network lifespan compared to the other protocols, with HLEACH leading the pack. However, the proposed model shows competitive performance, positioning higher in between HLEACH, SEP and the other protocols in terms of prolonging the network's operational duration.

In this case of scenario 1, also, the FND round is increased for all the protocols than the proposed but the other protocols failed to prolong the network lifetime due to improper protocol design. In this case, by the Tables 16 and 22, the clear performance of the proposed is better than the other compared protocols. In the scenario 2, the proposed model has higher energy efficiency, higher packet reception and longer network duration.

7) OVERALL NETWORK ANALYSIS

The proposed algorithm is further accessed with End-to-end delay, Throughput, Packet Reception Ratio and computational complexity.

a: AVERAGE ENERGY CONSUMPTION PER ROUND

Figure (21) presents the average energy consumption per round in all models, where each round encompasses sensing, processing, data aggregation, and communication activities, all drawing from the limited power sources of sensor nodes. Notably, the proposed model exhibits lower energy consumption compared to other models, despite occasional instances where its consumption surpasses that of MOBGWO and EEHCT. However, on an aggregate level, the proposed model demonstrates superior energy efficiency. Specifically in Figure (21a) of scenario 1, its overall average energy consumption exceeds HLEACH by 44.1%, SEP by 43.2%, MultiHet by 22.98%, MOBGWO by 14.11%, and EEHCT by 5.7%. It is clear that in scenario 2 of Figure (21b), that the energy consumption per node is totally increased from $450\mu J$ to 2000 μJ, but the proposed model is least among the other models in scenario 2. This emphasizes the efficacy of the proposed model in optimizing energy utilization across various WSN operations in scenario 1 and 2, promising enhanced longevity and sustainability for sensor network deployments.

b: PACKET RECEPTION RATIO

The Packet Reception Ratio (PRR) is a crucial metric in WSN, that quantifies the reliability of data transmission. PRR represents the proportion of successfully received packets relative to the total number of packets sent. PRR is calculated using the equation (35).

$$PRR = \frac{\sum No.of\ ReceivedPackets}{\sum No.of\ SentPackets} \times 100 \qquad (55)$$

The overall average PRR is plotted in figure 22 for all the cases of scenario 1 and scenario 2 analysis. In the average of all values, the MultiHet has the lowest PRR compared to other models, though the SEP is inefficient in Energy, and throughput but better in PRR. A high PRR of the proposed algorithm indicates robust and reliable communication as in Figure 20a is 0.9 which is reduced to the 0.85 in Figure 20b.

c: AVERAGE THROUGHPUT

The Throughput is a vital performance metric in networking that quantifies the amount of data successfully transmitted over a network or system within a given period. The average throughput in Figure 23 reflects the network's efficiency and

capacity, indicating how much useful data can be transferred in a specific timeframe. High throughput signifies a network's ability to handle a substantial volume of data quickly. The proposed model demonstrates an increase in throughput as node's initial energy increases in scenario 1, however the scenario 2 maximum average throughput is decreased to 0.22 and also for all the models when compared to scenario 1.

d: AVERAGE END TO END DELAY

At last, the End-to-End delay metric in networking measures the time it takes for a data packet to travel from the source (Node) to the destination (Base station), which includes the data processing, data aggregating and transmission time. The Average End-to-End delay in the network of 100 nodes and 200 nodes with all cases are given in Figure 24. Especially, HLEACH and SEP exhibit the lowest end-to-end delay in both scenarios, attributed to their direct transmission of data to the BS. Conversely, MOBGWO experiences a slightly higher delay due to its optimization in CH selection, which involves identifying the best optimal value and thus takes additional time. Following this, MultiHet demonstrates the next highest delay, owing to its weight-based CH selection approach, necessitating the calculation of fitness function values for each node, adding to the processing time. The highest delay is in EEHCT because initially EEHCT employs dynamic clustering based on Received Signal Strength Indicator (RSSI), similar to LEACH. However, it later transitions to static clusters based on energy balancing among nodes. This transition process and the overhead associated with maintaining static clusters could contribute to increased delay compared to LEACH, which may maintain dynamic clustering throughout its operation. Additionally, the introduction of temporary cluster heads (TCHs) in EEHCT to decide cluster heads for future rounds introduces additional complexity and potential delays in the cluster head selection process.

In the proposed model, the end-to-end delay is observed to be lower than that of EEHCT and, in certain scenarios, even MultiHet. However, it remains higher compared to other models, primarily due to the routing of data and the time required for network analysis using GNN. Unlike other models, the proposed approach acknowledges this delay as a limitation. The overall maximum delay observed in the scenario 1 is 1ms which is increased twice in the scenario 2 as 2ms.

e: COMPUTATIONAL COMPLEXITY

The proposed model involving the use of GNN for clustering nodes and electing eligible nodes for routing and best routing election, a significant limitation arises from the computational complexity of GNNs ($O(n^2)$), which scales quadratically with the number of nodes (n). This limitation impedes the scalability of the proposed algorithms and restricts their applicability to small-scale WSN deployments.

VI. CONCLUSION

This paper has proposed a distinctive clustering and cluster head selection algorithm for optimal cluster formation to enhance the pivotal challenges of energy efficiency and throughput in wireless sensor networks using the significance of GNN model.

The weight-based cluster head selection method has various processes but inducing the scale-based model is proposed in this paper that is applicable to all the weight-based cluster head selection protocols. This method evaluates the nodes individually in the cluster by distributed probability to rank the contender nodes to be designated as cluster heads with the fitness function. GraphSage routing model is is indulged in the progression of relay node selection with optimal path this escalates the energy efficiency. The obtained results of the multiple analyses through simulation that the proper method of clustering, cluster head selection and optimal routing would increase the network lifetime and the throughput by 24% on the calculated value of the last node dead in the network.

Future work can be on the application of weight-based cluster head selection with newer techniques and also to be implemented with the energy harvesting network in which the fitness function of residual energy will vary unpredictably. In this paper, the fitness functions and the routing strategies are related to static objective functions, which effectively addresses energy efficiency of static nodes for monitoring environmental changes in applications such as agricultural farmland and non-human operable areas. Therefore, the proposed model is not validated on the high mobility scenario. Thus, future work is essential to enhance the applicability in high mobility scenarios.

REFERENCES

[1] R. Ramya and D. T. Brindha, "A comprehensive review on optimal cluster head selection in WSN-IoT," *Adv. Eng. Softw.*, vol. 171, Sep. 2022, Art. no. 103170, doi: 10.1016/j.advengsoft.2022.103170.

[2] O. A. Amodu, U. A. Bukar, R. A. Raja Mahmood, C. Jarray, and M. Othman, "Age of information minimization in UAV-aided data collection for WSN and IoT applications: A systematic review," *J. Netw. Comput. Appl.*, vol. 216, Jul. 2023, Art. no. 103652, doi: 10.1016/j.jnca.2023.103652.

[3] R. Yadav, I. Sreedevi, and D. Gupta, "Augmentation in performance and security of WSNs for IoT applications using feature selection and classification techniques," *Alexandria Eng. J.*, vol. 65, pp. 461–473, Feb. 2023, doi: 10.1016/j.aej.2022.10.033.

[4] X. Zhao, Z. Qu, H. Tang, S. Tao, J. Wang, B. Li, and Y. Shi, "A detection probability guaranteed energy-efficient scheduling mechanism in large-scale WSN," *Alexandria Eng. J.*, vol. 71, pp. 451–462, May 2023, doi: 10.1016/j.aej.2023.03.059.

[5] B. A. Begum and S. V. Nandury, "Data aggregation protocols for WSN and IoT applications – a comprehensive survey," *J. King Saud Univ. - Comput. Inf. Sci.*, vol. 35, no. 2, pp. 651–681, Feb. 2023, doi: 10.1016/j.jksuci.2023.01.008.

[6] K. Guleria, A. K. Verma, N. Goyal, A. K. Sharma, A. Benslimane, and A. Singh, "An enhanced energy proficient clustering (EEPC) algorithm for relay selection in heterogeneous WSNs," *Ad Hoc Netw.*, vol. 116, May 2021, Art. no. 102473, doi: 10.1016/j.adhoc.2021.102473.

[7] K. S. Adu-Manu, F. Engmann, G. Sarfo-Kantanka, G. E. Baiden, and B. A. Dulemordzi, "WSN protocols and security challenges for environmental monitoring applications: A survey," *J. Sensors*, vol. 2022, pp. 1–21, Aug. 2022, doi: 10.1155/2022/1628537.

[8] R. M. Gomathi and J. M. L. Manickam, "Energy efficient shortest path routing protocol for underwater acoustic wireless sensor network," *Wireless Pers. Commun.*, vol. 98, no. 1, pp. 843–856, Jan. 2018, doi: 10.1007/s11277-017-4897-5.

[9] S. Chaurasia, K. Kumar, and N. Kumar, "MOCRAW: A meta-heuristic optimized cluster head selection based routing algorithm for WSNs," *Ad Hoc Netw.*, vol. 141, Mar. 2023, Art. no. 103079, doi: 10.1016/j.adhoc.2022.103079.

[10] A. Shahraki, A. Taherkordi, Ø. Haugen, and F. Eliassen, "Clustering objectives in wireless sensor networks: A survey and research direction analysis," *Comput. Netw.*, vol. 180, Oct. 2020, Art. no. 107376, doi: 10.1016/j.comnet.2020.107376.

[11] K. Deb and K. Deb, "Multi-objective optimization," in *Nature-Inspired Optimization Algorithms*. Amsterdam, The Netherlands: Elsevier, 2013, pp. 403–449.

[12] D. Sharma, A. Ojha, and A. P. Bhondekar, "Heterogeneity consideration in wireless sensor networks routing algorithms: A review," *J. Supercomput.*, vol. 75, no. 5, pp. 2341–2394, May 2019, doi: 10.1007/s11227-018-2635-8.

[13] O. Beaumont, B. A. Becker, A. DeFlumere, L. Eyraud-Dubois, T. Lambert, and A. Lastovetsky, "Recent advances in matrix partitioning for parallel computing on heterogeneous platforms," *IEEE Trans. Parallel Distrib. Syst.*, vol. 30, no. 1, pp. 218–229, Jan. 2019, doi: 10.1109/TPDS.2018.2853151.

[14] S. Jabbehdari and A. Khadem-Zadeh, "Comparison of energy efficient clustering protocols in heterogeneous wireless sensor networks," *Int. J. Adv. Sci. Technol.*, vol. 7, pp. 1–20, Apr. 2011.

[15] S. Singh, "Energy efficient multilevel network model for heterogeneous WSNs," *Eng. Sci. Technol., Int. J.*, vol. 20, no. 1, pp. 105–115, Feb. 2017.

[16] N. Sharma and V. R. Verma, "Heterogeneous LEACH protocol for wireless sensor networks," *Int. J. Adv. Netw. Appl.*, vol. 5, pp. 1825–1829, Jan. 2013.

[17] M. Tong and M. Tang, "LEACH-B: An improved LEACH protocol for wireless sensor network," in *Proc. 6th Int. Conf. Wireless Commun. Netw. Mobile Comput. (WiCOM)*, Chengdu City, China, Sep. 2010, pp. 1–4, doi: 10.1109/WICOM.2010.5601113.

[18] Z. Beiranvand, A. Patooghy, and M. Fazeli, "I-LEACH: An efficient routing algorithm to improve performance & to reduce energy consumption in wireless sensor networks," in *Proc. 5th Conf. Inf. Knowl. Technol.*, shiraz, Iran, May 2013, pp. 13–18, doi: 10.1109/IKT.2013.6620030.

[19] A. Mehmood, J. Lloret, M. A. Noman, and H. Song, "Improvement of the wireless sensor network lifetime using LEACH with vice-cluster head," *Ad Hoc Sens. Wireless Netw.*, vol. 28, pp. 1–17, Jan. 2015.

[20] L. Aziz, "A new enhanced version of VLEACH protocol using a smart path selection," *Int. J. GEOMATE*, vol. 12, no. 30, pp. 28–34, Feb. 2017.

[21] W. Neji, S. B. Othman, and H. Sakli, "T-LEACH: Threshold sensitive low energy adaptive clustering hierarchy for wireless sensor networks," in *Proc. 20th Int. Conf. Sci. Techn. Autom. Control Comput. Eng. (STA)*, Monastir, Tunisia, Dec. 2020, pp. 336–342.

[22] H. Junping, J. Yuhui, and D. Liang, "A time-based cluster-head selection algorithm for LEACH," in *Proc. IEEE Symp. Comput. Commun.*, Jul. 2008, pp. 1172–1176, doi: 10.1109/ISCC.2008.4625714.

[23] O. Younis and S. Fahmy, "HEED: A hybrid, energy-efficient, distributed clustering approach for ad hoc sensor networks," *IEEE Trans. Mobile Comput.*, vol. 3, no. 4, pp. 366–379, Oct. 2004, doi: 10.1109/TMC.2004.41.

[24] G. Smaragdakis, I. Matta, and A. Bestavros, "SEP: A stable election protocol for clustered heterogeneous wireless sensor networks," in *Proc. 2nd Int. Workshop Sensor Actor Netw. Protocols Appl.*, May 2004, pp. 1–20.

[25] S. Chand, S. Singh, and B. Kumar, "Heterogeneous HEED protocol for wireless sensor networks," *Wireless Pers. Commun.*, vol. 77, no. 3, pp. 2117–2139, Aug. 2014, doi: 10.1007/s11277-014-1629-y.

[26] S. Singh, A. Malik, and R. Kumar, "Energy efficient heterogeneous DEEC protocol for enhancing lifetime in WSNs," *Eng. Sci. Technol., Int. J.*, vol. 20, no. 1, pp. 345–353, Feb. 2017.

[27] Z. Fan and H. Zhou, "A distributed weight-based clustering algorithm for WSNs," in *Proc. Int. Conf. Wireless Commun., Netw. Mobile Comput.*, Sep. 2006, pp. 1–5, doi: 10.1109/WiCOM.2006.275.

[28] S. K. Chaurasiya, S. Mondal, A. Biswas, A. Nayyar, M. A. Shah, and R. Banerjee, "An energy-efficient hybrid clustering technique (EEHCT) for IoT-based multilevel heterogeneous wireless sensor networks," *IEEE Access*, vol. 11, pp. 25941–25958, 2023, doi: 10.1109/ACCESS.2023.3254594.

[29] L. Sahoo, S. Supriyan Sen, K. Tiwary, S. Moslem, and T. Senapati, "Improvement of wireless sensor network lifetime via intelligent clustering under uncertainty," *IEEE Access*, vol. 12, pp. 25018–25033, 2024, doi: 10.1109/ACCESS.2024.3365490.

[30] H. Han, J. Tang, and Z. Jing, "Wireless sensor network routing optimization based on improved ant colony algorithm in the Internet of Things," *Heliyon*, vol. 10, no. 1, Jan. 2024, Art. no. e23577, doi: 10.1016/j.heliyon.2023.e23577.

[31] S. D. Mishra and D. Verma, "Energy-efficient and reliable clustering with optimized scheduling and routing for wireless sensor networks," *Multimedia Tools Appl.*, vol. 83, no. 26, pp. 68107–68133, Mar. 2024.

[32] G. A. Senthil, A. Raaza, and N. Kumar, "Internet of Things energy efficient cluster-based routing using hybrid particle swarm optimization for wireless sensor network," *Wireless Pers. Commun.*, vol. 122, no. 3, pp. 2603–2619, Feb. 2022, doi: 10.1007/s11277-021-09015-9.

[33] P. Ding, J. Holliday, and A. Celik, "Distributed energy-efficient hierarchical clustering for wireless sensor networks," in *Distributed Computing in Sensor Systems*. Springer, 2005, pp. 322–339.

[34] H. Hu, X. Fan, C. Wang, T. Wang, and Y. Deng, "Particle swarm optimization and fuzzy logic based clustering and routing protocol to enhance lifetime for wireless sensor networks," *Cluster Comput.*, vol. 27, no. 7, pp. 9715–9734, Oct. 2024, doi: 10.1007/s10586-024-04453-z.

[35] L. Yuebo, Y. Haitao, L. Hongyan, and L. Qingxue, "Fuzzy clustering and routing protocol with rules tuned by improved particle swarm optimization for wireless sensor networks," *IEEE Access*, vol. 11, pp. 128784–128800, 2023, doi: 10.1109/ACCESS.2023.3332914.

[36] R. Pal, M. Saraswat, S. Kumar, A. Nayyar, and P. K. Rajput, "Energy efficient multi-criterion binary grey wolf optimizer based clustering for heterogeneous wireless sensor networks," *Soft Comput.*, vol. 28, no. 4, pp. 3251–3265, Feb. 2024, doi: 10.1007/s00500-023-09316-0.

[37] M. Lin, W. Xu, Z. Lin, and R. Chen, "Determine OWA operator weights using kernel density estimation," *Econ. Research-Ekonomska Istraživanja*, vol. 33, no. 1, pp. 1441–1464, Jan. 2020.

[38] Z. Liu, X. Mou, H.-C. Liu, and L. Zhang, "Failure mode and effect analysis based on probabilistic linguistic preference relations and gained and lost dominance score method," *IEEE Trans. Cybern.*, vol. 53, no. 3, pp. 1566–1577, Mar. 2023, doi: 10.1109/TCYB.2021.3105742.

[39] L. D. Hopkins, "Multi-attribute decision making in urban studies," in *International Encyclopedia of the Social Behavioral Sciences*. Oxford, U.K.: Pergamon, 2001, pp. 10157–10160, doi: 10.1016/B0-08-043076-7/04437-5.

[40] V. Rajput and A. C. Shukla, "Decision-making using the analytic hierarchy process (AHP)," *Int. J. Scientific Res.*, vol. 3, no. 6, pp. 135–136, Jun. 2012.

[41] A. Ullah, F. S. Khan, Z. Mohy-ud-din, N. Hassany, J. Z. Gul, M. Khan, W. Y. Kim, Y. C. Park, and M. M. Rehman, "A hybrid approach for energy consumption and improvement in sensor network lifespan in wireless sensor networks," *Sensors*, vol. 24, no. 5, p. 1353, Feb. 2024, doi: 10.3390/s24051353.

[42] K. C. Y and S. B. M, "An improvised dual step hybrid routing protocol for network lifetime enhancement in WSN-IoT environment," *Multimedia Tools Appl.*, vol. 83, no. 21, pp. 59965–59984, Jan. 2024.

[43] S. He, S. Xiong, Y. Ou, J. Zhang, J. Wang, Y. Huang, and Y. Zhang, "An overview on the application of graph neural networks in wireless networks," *IEEE Open J. Commun. Soc.*, vol. 2, pp. 2547–2565, 2021, doi: 10.1109/OJCOMS.2021.3128637.

[44] T. Zhu, X. Chen, L. Chen, W. Wang, and G. Wei, "GCLR: GNN-based cross layer optimization for multipath TCP by routing," *IEEE Access*, vol. 8, pp. 17060–17070, 2020, doi: 10.1109/ACCESS.2020.2966045.

[45] H. Li, W. Dong, Y. Wang, Y. Gao, and C. Chen, "Enhancing the performance of 802.15.4-based wireless sensor networks with NB-IoT," *IEEE Internet Things J.*, vol. 7, no. 4, pp. 3523–3534, Apr. 2020.

[46] W. B. Heinzelman, A. P. Chandrakasan, and H. Balakrishnan, "An application-specific protocol architecture for wireless microsensor networks," *IEEE Trans. Wireless Commun.*, vol. 1, no. 4, pp. 660–670, Oct. 2002, doi: 10.1109/TWC.2002.804190.

[47] L. Qing, Q. Zhu, and M. Wang, "Design of a distributed energy-efficient clustering algorithm for heterogeneous wireless sensor networks," *Comput. Commun.*, vol. 29, no. 12, pp. 2230–2237, Aug. 2006, doi: 10.1016/j.comcom.2006.02.017.
[48] P. Cunningham and S. J. Delany, "K-nearest neighbour classifiers—A tutorial," *ACM Comput. Surveys*, vol. 54, no. 6, pp. 1–25, Jul. 2022, doi: 10.1145/3459665.
[49] R. L. Graham and P. Hell, "On the history of the minimum spanning tree problem," *IEEE Ann. Hist. Comput.*, vols. AHC-7, no. 1, pp. 43–57, May 1985, doi: 10.1109/MAHC.1985.10011.
[50] W. L. Hamilton, R. Ying, and J. Leskovec, "Inductive representation learning on large graphs," in *Proc. 31st Conf. Neural Inf. Process. Syst. (NIPS)*, Long Beach, CA, USA, Jan. 2017, pp. 1024–1034.
[51] S. M. M. H. Daneshvar and S. M. Mazinani, "On the best fitness function for the WSN lifetime maximization: A solution based on a modified salp swarm algorithm for centralized clustering and routing," *IEEE Trans. Netw. Service Manage.*, vol. 20, no. 4, pp. 4244–4254, Dec. 2023.
[52] V. Jha and R. Sharma, "An energy efficient weighted clustering algorithm in heterogeneous wireless sensor networks," *J. Supercomput.*, vol. 78, no. 12, pp. 14266–14293, Aug. 2022, doi: 10.1007/s11227-022-04429-z.
[53] M. Saadati, S. M. Mazinani, A. A. Khazaei, and S. J. S. M. Chabok, "Energy efficient clustering for dense wireless sensor network by applying graph neural networks with coverage metrics," *Ad Hoc Netw.*, vol. 156, Apr. 2024, Art. no. 103432.

R. BLESSINA PREETHI is currently with Vellore Institute of Technology (VIT), Chennai, India, as a Research Scholar. With a fervent passion for advancing technological frontiers, her recent focus lies at the intersection of wireless sensor networks and the Internet of Things (IoT). Her pioneering research endeavors revolve around energy efficiency within these domains through the adept application of cutting-edge machine-learning models.

M. SARANYA NAIR received the B.E. degree in electronics and communication engineering and the M.E. degree in communication and networking from Anna University, in 2008 and 2010, respectively, and the Ph.D. degree in electronics engineering from VIT, Chennai, in 2020. She is currently an Associate Professor with the School of Electronics Engineering, VIT University, Chennai Campus, has 13 years of teaching experience, including research experience in wireless sensor networks, cellular networks, underwater networks, and the IoT in healthcare. During the Ph.D. degree, she has proposed an efficient time synchronization algorithm for underwater acoustic wireless sensor networks. Her areas of specialization are wireless sensor networks—applications and protocol design, underwater acoustic wireless sensor networks, the IoT in healthcare & industry 4.0, cellular networks—energy optimization in 5G and beyond, and energy harvesting and management. She has published more than 25 research publications in reputed journals and contributed for more than ten books in Springer and Elsevier and Wiley.